

**SCHOOL OF MATERIALS AND MINERAL RESOURCES ENGINEERING  
UNIVERSITI SAINS MALAYSIA**

**MICROSTRUCTURE EVOLUTION OF ISOTHERMALLY AGED ECAPED  
SAC SOLDER ALLOY**

By

**NUR AMIERA BINTI ZULKIFLI**

**Supervisor : Assoc. Prof. Dr. Nurulakmal binti Mohd. Sharif**

Dissertation submitted in partial fulfillment  
of the requirements for the degree of Bachelor of Engineering with Honours  
(Materials Engineering)

Universiti Sains Malaysia

**JULY 2017**

## DECLARATION

I hereby declare that I have conducted, completed the research work and written the dissertation entitled “**MICROSTRUCTURE EVOLUTION OF ISOTHERMALLY AGED ECAPED SAC SOLDER ALLOY**”. I also declared that it has not been previously submitted for the award or any degree or diploma or other similar title of this for any other examining body of University.

Name of Student : Nur Amiera binti Zulkifli

Signature:

Date : 4 JULY 2017

Witness by

Supervisor : Assoc. Prof. Dr. Nurulakmal binti Mohd. Sharif

Signature:

Date : 4 JULY 2017

## **ACKNOWLEDGEMENTS**

After undergone countless of efforts and discussions, Alhamdulillah praise to Allah for giving me strength and guidance to me in completing my final year project as partial fulfillment of the requirement to graduate. First and foremost, I would like to express my gratitude to my project's supervisor, Assoc. Prof. Dr. Nurulakmal binti Mohd. Sharif for giving me suggestions and advices as well as encouragements along the project. This project would not be completed without the help from my supervisor.

I would like to thank to all the technicians who involve in helping me to carry out the experimental work during this project. Their contributions in giving great services are very helpful and useful for me to finish my project. They also helping me in giving some suggestions and solutions on the problems that I face during handling experimental work in lab.

Moreover, my special thanks to the authority of Universiti Sains Malaysia (USM) especially to School of Material and Mineral Resources Engineering for providing me with all the facilities needed to complete this project. Next, I also would like to thank to my parents for always giving advice and encouragement whenever I have problems. Last but not least, I would like to thank all the people who involved directly or indirectly in helping me during the project.

## TABLE OF CONTENTS

<b>Contents</b>	<b>Page</b>
DECLARATION	ii
ACKNOWLEDGEMENT	iii
LIST OF TABLES	vii
LIST OF FIGURES	viii
LIST OF ABBREVIATIONS	xi
LIST OF SYMBOLS	xiv
ABSTRAK	xv
ABSTRACT	xvii
<b>CHAPTER 1 INTRODUCTION</b>	<b>1</b>
1.1 Background of Study	1
1.2 Problem statement	4
1.3 Objective	5
1.4 Scope of Study	6
<b>CHAPTER 2 LITERATURE REVIEW</b>	<b>7</b>
2.1 Solder Alloys	7
2.1.1 Properties of solder	9
2.1.2 Sn-Ag-Cu Solder Alloys	11
2.1.3 Modification in Microstructure of Sn-based Solder Alloys	14

2.2	Theory of Severe Plastic Deformation (SPD) Techniques	15
2.2.1	Formation of Ultra-fine Grains (UFG)	17
2.2.2	High Angle Grain Boundaries (HAGB)	18
2.3	Concept of Equal Channel Angular Pressing (ECAP)	20
2.3.1	Principles of Equal Channel Angular Pressing (ECAP)	21
2.3.2	Evaluations of Strain obtained during ECAP	22
2.3.3	Types of Equal Channel Angular Pressing (ECAP)	24
2.3.4	Microstructure Evolution during ECAP	25
2.4	Characterization of Solder Materials	25
2.4.1	Wettability	26
2.4.2	Mechanical Properties of Solder Joint	27
2.4.3	Intermetallic Compound (IMC) formation	30
	<b>CHAPTER 3 MATERIALS AND EXPERIMENTAL PROCEDURES</b>	<b>35</b>
3.1	Materials and experimental procedures	35
3.2	Materials	36
3.3	Equal Channel Angular Pressing (ECAP) Processing	38
3.4	Reflow Process	41
3.5	Isothermal aging	42
3.6	Mechanical Properties Testing	42
3.6.1	Microhardness Testing	42

3.6.2	Tensile testing	43
3.7	Characterization	44
3.7.1	Scanning Electron Microscopy (SEM)	44
3.7.2	X-ray Fluorescence (XRF)	45
3.7.3	Optical Microscopy (OM)	45
3.7.4	Stereo Zoom Microscope	47
<b>CHAPTER 4 RESULTS AND DISCUSSION</b>		<b>49</b>
4.1	Overview	
4.2	Microstructure Evolution of Sn-Ag-Cu Solder Alloy	49
4.2.1	Microstructure of Bulk ECAPed Solder Alloy	49
4.2.2	Grain Size Measurement	51
4.2.3	Comparison of Microstructure of ECAPed Bulk Solder with Different Routes	54
4.3	Wettability of Reflowed ECAPed Sn-Ag-Cu Solder Alloy	56
4.4	Spreading Test	56
4.5	Microhardness of ECAPed Solder Alloy	58
4.6	Isothermal Aging	60
4.7	Tensile Strength	66

<b>CHAPTER 5 CONCLUSION AND RECOMMENDATIONS</b>	69
5.1 Conclusion	69
5.2 Recommendation	70
<b>REFERENCES</b>	72

## LIST OF TABLES

Table 1.1 : Melting points of common solder elements	1
Table 2.1 : Major lead-free candidates for replacing traditional Sn-Pb solder alloys	12
Table 2.2 Effect of various nanoparticles addition into the lead free solder paste on melting temperature	33
Table 3.1 : Chemical composition of SAC 305 solder alloy	37
Table 4.1 : Average grain size of solder alloy after ECAP pressing with different number of pass	53
Table 4.2 : Optical microscopy images of bulk ECAPed solder alloy of route A and route Bc 0 pass, 4 passes and 9 passes	55
Table 4.3 : Wetting angles of ECAPed solder alloys	
Table 4.4 : Length and width of reflowed solder on Cu substrate	57
Table 4.5 : Vickers hardness reading (Hv) for route A	58
Table 4.6 : Vickers hardness reading (Hv) for route B <sub>c</sub>	59
Table 4.7 : Thickness of IMC layer for as-reflowed sample and after isothermal aging	60
Table 4.8 : Tensile strength (MPa)of ECAPed solder alloy before aging	65
Table 4.9 : Tensile strength (MPa) of ECAPed solder alloy after aging	66



## LIST OF FIGURES

Figure 1.1 : The schematic of solder bump for a flip-chip interconnect in electronic packaging	2
Figure 1.2 : An optical micrograph of the microstructure of Sn-3.8Ag-0.3Cu solder in a flip-chip bump on a copper UBM	3
Figure 2.1 : Schematic of solder joint in electronic packaging	8
Figure 2.2 : Schematic of structure of solder joint and its failure modes	8
Figure 2.3 : Spreading of a liquid with negligible vapor pressure on a solid surface S	10
Figure 2.4 : Phase diagram of SAC alloy	13
Figure 2.5 : Several processes in SPD, (a) Equal Channel Angular Pressing (ECAP) (b) High Pressure Torsion (HPT) (c) Accumulative Roll Bonding (ARB) (d) Reciprocating Extrusion-Compression (REC) (e) Cyclic Close Die Forging (CCDF) and (f) Repetitive Corrugation and Straightening (RCS)	16
Figure 2.6 : The formation of UFG by ECAP (a) before ECAP (b) after ECAP	18
Figure 2.7 : High angle grain boundaries (HAGB) of pure Cu	19
Figure 2.8 : Example of microstructure of regular material and ultrafine-grained metal material	21
Figure 2.9 : Schematic representation of SPD processes in terms of strain distribution	23
Figure 2.10 : Types of billet rotation between consecutive passes through	24

ECAP die tool

Figure 2.11 : Schematic of wetting and non wetting solder	26
Figure 2.12 : Example of IMC layer which composed of $Ag_3Sn$ and $Cu_6Sn_5$ compounds	31
Figure 2.13 Thermal fatigue cracks initiate and propagate through intermetallics layer of Sn-Ag-Cu solder	31
Figure 3.1 : Flowchart of experimental procedures	36
Figure 3.2 : Heating profile of SAC solder alloy	38
Figure 3.3 : Processing of equal channel angular pressing (ECAP)	39
Figure 3.4 : Route A in ECAP processing	40
Figure 3.5 Route Bc in ECAP processing	40
Figure 3.6 : Reflowed solder sheet embedded on Cu substrate	41
Figure 3.7 : Schematic representation of Vickers hardness indentation	43
Figure 3.8 : Lap joint for shear test	44
Figure 3.9 : Definition of the parameters to characterize the IMC microstructure	46
Figure 3.10 Stereo Zoom Microscope	47
Figure 3.11 Measurement of diameter of reflowed solder on Cu substrate	48
Figure 4.1 : SEM microstructure of ECAPed solder alloy with (a) 0 pass (b) 4 passes and (c) 9 passes	50
Figure 4.2 : Scanning electron microscopy images used in the measurement of grain size of solder alloy with different number of ECAP passes (a) 0 pass (b) 4 passes and (c) 9 passes	53

Figure 4.3 : IMC layer at solder-substrate interface for reflowed samples, (a) 0 pass (b) 4 passes and (c) 9 passes ECAPed solder alloys	61
Figure 4.4 : IMC layer at solder-substrate interface for isothermally aged for 100 hours at 180°C samples, (a) 0 pass (b) 4 passes and (c) 9 passes ECAPed solder alloys	62
Figure 4.5 : IMC layer at solder-substrate interface for isothermally aged for 250 hours at 180°C samples, (a) 0 pass (b) 4 passes and (c) 9 passes ECAPed solder alloys	63
Figure 4.6 : IMC layer at solder-substrate interface for isothermally aged for 500 hours at 180°C samples, (a) 0 pass (b) 4 passes and (c) 9 passes ECAPed solder alloys	64
Figure 4.7 : Scanning electron microscopy images on the fracture surface of solder joint after shear test	67
Figure 4.8 : Surface morphology on fracture surface of reflowed solder during tensile test for different ECAP passes (a) 0 pass (b) 4 passes (c) 9 passes	68

## LIST OF ABBREVIATIONS

Sn	Tin
Pb	Lead
Ag	Silver
Bi	Bismuth
In	Indium
Sb	Antimony
Cd	Cadmium
Sn-Pb	Tin-lead
Sn-Ag	Tin-silver
Sn-Cu	Tin-copper
Sn-Bi	Tin-bismuth
Sn-Zn	Tin-zinc
Sn-Ag-Cu	Tin-silver-copper
Sn-Ag-Bi	Tin-silver-bismuth
Ni	Nickel
Co	Cobalt

Fe	Ferum
Mn	Manganese
Zn	Zinc
Ti	Titanium
Ce	Cerium
Al	Aluminium
ECAP	Equal Channel Angular Pressing
IMC	Intermetallic compound
SAC	Sn-Ag-Cu
UFG	Ultra-fine grain
SPD	Severe Plastic Deformation
T	Temperature
P	Pressure
G	Free energy
A	Area
S	Solid
RoHS	Restriction of use Hazardous Substances

HPT	High Pressure Torsion
ARB	Accumulative Roll Bonding
REC	Reciprocating Extrusion-Compression
CCDF	Cyclic Close Die Forging
RCS	Repetitive Corrugation and Straightening
HAGB	High Angle Grain Boundaries
FE-SEM	Field Emission Scanning Electron Microscopy
EDX	Energy Dispersive X-ray spectroscopy
UTM	Universal Testing Machine
SiC	Silicon Carbide
RA	Activated Rosin
OM	Optical Microscopy

## LIST OF SYMBOLS

$G$	Free Energy
$A$	Area
$\Gamma$	Surface Tension
$\Gamma_{ls}$	Liquid-Solid Surface Tension
$\Gamma_{vl}$	Vapour-Liquid Surface Tension
$\Gamma_{sv}$	Solid-Vapour Surface Tension
$\Phi$	Die Angle
$\Psi$	Curvature Angle
$T$	Temperature
$T_m$	Melting Temperature

# **PERUBAHAN MIKROSTRUKTUR SAC PATERI YANG MELALUI PROSES ECAP DAN PENUAAN ISOTERMA**

## **ABSTRAK**

Beberapa tahun kebelakangan ini, Sn-Ag-Cu pateri aloi sesuai untuk menggantikan pateri konvensional timah plumbum (Sn-Pb). Walaupun pateri SAC mempunyai kelebihan, permintaan semasa lebih memilih pateri yang bersifat mekanikal yang mampu menyediakan reliabiliti kepada penyambung pateri. Dalam projek ini, pendekatan plastik ubah bentuk iaitu teknik Penekanan melalui Saluran yang Mempunyai Sudut yang Sama (ECAP) akan digunakan pada SAC 305 pateri untuk meningkatkan sifat-sifat mekanikal. Tumpuan adalah kepada pengaruh ECAP melalui penghalusan bijian kepada tingkah laku IMC semasa penuaan isoterma. Pencirian aloi pateri tertumpu kepada mikrostruktur solder pukal, lapisan IMC di penyambung pateri semasa proses penyambungan dan pertumbuhan IMC semasa penuaan isoterma. Proses penyambungan dilakukan pada 270°C manakala penuaan telah dijalankan secara isoterma pada suhu 180°C selama 100 jam, 250 jam dan 500 jam. Mikrostruktur pukal pateri dan IMC terbentuk diperhatikan menggunakan FE-SEM dilengkapi dengan EDX. Kekerasan pateri pukal diukur melalui alat mikro Vickers kekerasan manakala kekuatan tegangan penghubung solder dinilai menggunakan ujian kekuatan ricih penyambung. Pemrosesan ECAP dengan laluan A menyebabkan dendrit  $\beta$ -Sn panjang dan nipis manakala laluan Bc menghasilkan dendrit  $\beta$ -Sn halus yang sama. Kekerasan solder meningkat dengan bilangan ulangan ECAP manakala ketebalan lapisan IMC pateri menurun apabila bilangan ulangan ECAP tinggi. Sampel penuaan isoterma dengan laluan A menunjukkan lapisan IMC tebal apabila masa penuaan yang lebih lama.



ECAP dengan 9 ulangan mempunyai kekuatan tegangan terendah kerana kehadiran banyak liang dalam penghubung pateri.

# **MICROSTRUCTURE EVOLUTION OF ISOTHERMALLY AGED ECAPED SAC SOLDER ALLOY**

## **ABSTRACT**

In recent years, Sn-Ag-Cu solder alloy has been found to be amongst the suitable candidate for replacement of the conventional tin-lead (Sn-Pb) solder. Despite the advantages of SAC solder, the current demand of interconnect material prefers a higher mechanical properties of solder which would provide higher reliability of solder joint. In this project, a severe plastic deformation approach, namely an Equal Channel Angular Pressing (ECAP) technique used on SAC 305 solder in order to increase mechanical properties. The focus is on the influence of ECAP grain refinement to the IMC behaviour during isothermal aging. Characterization of the solder alloys focused on microstructure of bulk solder, IMC layer at solder joint during reflow and IMC growth during isothermal aging. The reflow process was done at 270°C whereas aging was performed isothermally at 180°C for 100 hours, 250 hours and 500 hours. Microstructure of bulk solder and the interfacial IMC formed were observed using FE-SEM equipped with EDX. Hardness of the bulk solder was measured via micro Vickers hardness tester whereas tensile strength of solder joint was evaluated using a lap joint shear test. ECAP processing with route A resulted in elongated and thin  $\beta$ -Sn dendrites while route B<sub>c</sub> produced fine equiaxed  $\beta$ -Sn dendrites. The hardness of solder increased with number of ECAP passes while the IMC layer of solder joint decreased with higher number of passes. Isothermally aged samples with route A showed thicker IMC layer when the aging time is longer. ECAP with 9 passes possessed the lowest tensile strength due to the presence of many pores in solder joint.

# CHAPTER 1

## INTRODUCTION

### 1.1 Background of study

Solders are metal alloys used in joining and bonding of two or more components. They are described as fusible alloys with liquidus temperature below 400°C (Hwang et al. 2004). Generally, several elements which commonly used in solder alloys are tin (Sn), lead (Pb), silver (Ag), bismuth (Bi), indium (In), antimony (Sb), and cadmium (Cd) (Hwang, 2012) Table 1.1 illustrates the melting points for the elements.

Table 1.1 Melting points of common solder elements (Hwang, 2012)

Elements Melting point	Sn	Pb	Ag	Bi	In	Sb	Cd
°C	232	328	961	271.5	156.6	630.5	321.2

Solder usually applied in forms of molten state and other various physical forms, including ingot, bar, and powder. There are several criterias in selecting the solder alloy. Firstly, the range of melting point and mechanical properties should be related to the service temperature and conditions. Secondly, potential of formation of intermetallic compounds also must be taken into consideration as it may affects the solder joint. Thirdly, wettability

of solder alloy on specified substrate is also important in selecting solder alloy (Hwang et al. 2004).

In electronic industry, the solder was used to assemble all electronic components on substrate pad. Figure 1.1 shows the schematic of solder bump for a flip-chip interconnect in electronic packaging and Figure 1.2 shows the microstructure of Sn-3.8Ag-0.3Cu solder in a flip-chip bump on a copper UBM. The solder is usually melted and solidified creating a metal joint in order to produce an electrical connection by using thermosonic bonding or alternatively reflow process.

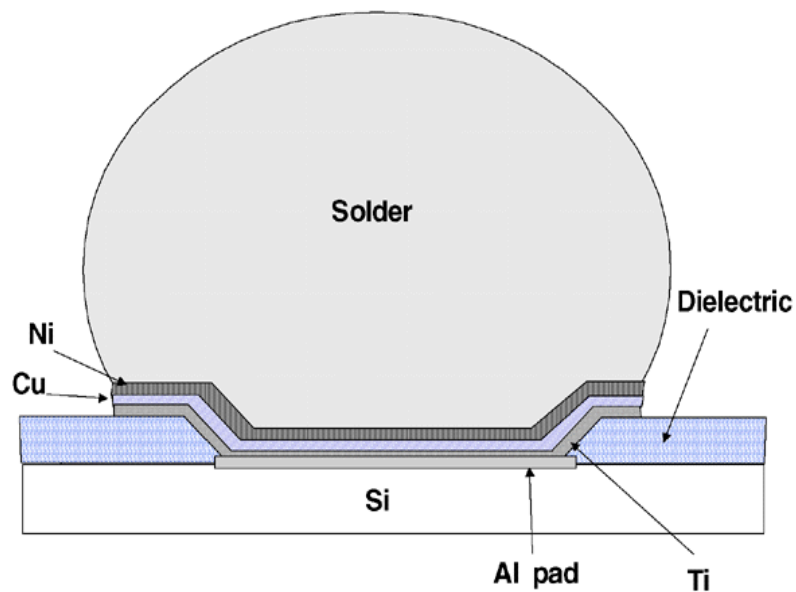


Figure 1.1 The schematic of solder bump for a flip-chip interconnect in electronic packaging (Frear, 1999).

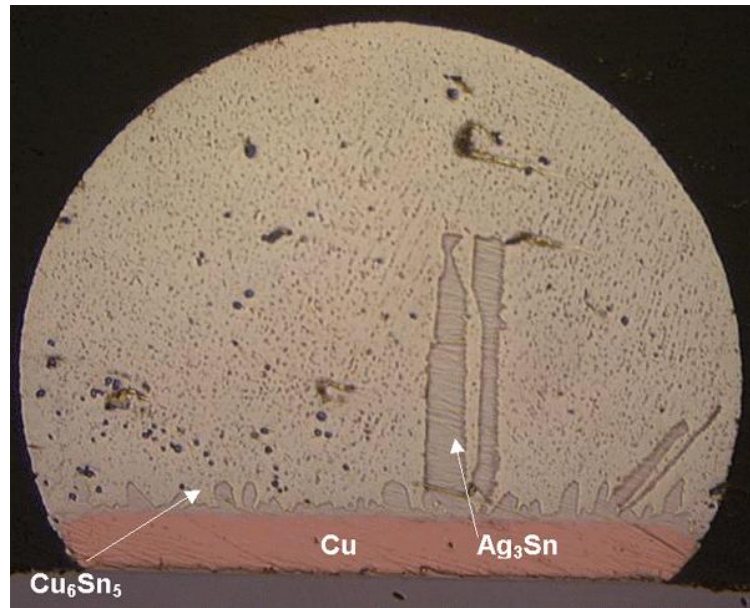


Figure 1.2 An optical micrograph of the microstructure of Sn-3.8Ag-0.3Cu solder in a flip-chip bump on a copper UBM (Frear et al. 2001).

Sn-Pb solder alloys are the most common solder materials used in electronic application because of their excellent properties. Eutectic Sn-Pb solder alloys have excellent wettability, low melting point and good mechanical properties. However, due to the toxicity and health concern of lead, Sn-Pb can no longer be in electronic devices (Gao et al. 2010). Therefore, new lead-free solders especially Sn-based alloys were developed for electronic application. Nowadays, the lead-free candidates which are under consideration are Sn-Ag, Sn-Cu, Sn-Bi, Sn-Zn, Sn-Ag-Cu and Sn-Ag-Bi (Karl and Kathleen 2004). Alternative Sn-Ag-Cu solder alloy is usually being proposed to be amongst the first candidates for replacing traditional Sn-Pb solder alloys. Sn-Ag-Cu solder alloys have

several advantages such as low melting temperature compared with Sn-Ag binary eutectic alloy, superior mechanical properties and good solderability (Kim et al. 2003).

## **1.2 Problem statement**

Despite the advantages of Sn-Ag-Cu, there are several issues with Sn-Ag-Cu that must be taken into consideration. Firstly, eutectic Sn-Ag-Cu has a melting temperature of 217°C and it may not be suitable for many temperature-sensitive applications. Secondly, the formation of large brittle intermetallic compounds (IMCs) as primary precipitates. There are two kinds of IMCs layer which may be formed in this solder alloy which are  $\text{Ag}_3\text{Sn}$  and  $\text{Cu}_6\text{Sn}_5$  depending on the phase diagram. Thirdly, Sn-Ag-Cu solder alloy also has poor fatigue characteristics (Kim et al. 2003). Therefore, researchers were trying to find suitable solution in order to improve the properties of this solder alloy. One of the methods which is usually used by researchers is by adding alloying elements into compositions of solder alloy such as Ni, Co, Fe, Mn, Zn, Ti, Ce, In and Al (Piyavatin et al. 2012). However, certain alloying elements could not give the required properties to solder alloy. For example, alloying elements such as Ni and Sb do not reduce the melting temperature of Sn-based solders but only added to enhance properties (Karl and Kathleen 2004). In addition, a research has studied on micro-alloying as an effective method to modify the properties of lead-free solder alloys, but adding of these elements also could affect their microstructure and other properties (El-Daly et al. 2013). Another method that can be used to improve the mechanical properties is by applying a severe plastic deformation to the solder alloy. The severe plastic deformation technique which is

commonly used is Equal Channel Angular Pressing (ECAP). This method can improve the mechanical properties of metal alloy by modifying the microstructure of metal alloy (Shaeri et al. 2015). The improvements can be seen through its mechanical properties of tensile strength, shear strength, creep resistance and impact resistance. The modification of microstructure of solder alloy involving the refining of grain size and concealing the formation of brittle IMC (Leong et al. 2016). Refinement of grain size and re-distribution of IMC could potentially enhance fatigue resistance of the solder.

### **1.3 Objective**

In this project, ECAP technique is used in order to improve the mechanical properties of SAC 305 (Sn-3.0Ag-0.5Cu). The microstructure was evaluated after several passes of ECAP (0, 4 and 9 passes) and growth of IMC layer at solder/substrate interface was assessed following isothermal aging of 180°C for 100 hours, 250 hours and 500 hours. Considering the above mentioned problem, a few objectives are set in order to improve the mechanical properties of solder alloy by applying an ECAP method. The research objectives involved in this study is

- 1) To analyse the effect of ECAP on bulk microstructure of SAC solder alloy
- 2) To evaluate the effect of ECAP on the microstructure changes and IMC growth during isothermal aging

## **1.4 Scope of study**

The material used in this research is Sn-Ag-Cu solder alloy. Due to drawbacks that may influence the properties of the solder alloy, a severe plastic deformation called ECAP is used in order to improve the mechanical properties. ECAP modifies the microstructure of solder alloy by refining the grain size and creates an ultra-fine grain (UFG). This effective method improves the mechanical properties of materials with respect to the grain size reduction. From the study, it is expected that during ECAP process, ECAP will improve the properties of solder which observed from microstructure changes of bulk solder alloy. Besides, ECAP is also expected to give effects on microstructure changes and IMC growth during isothermal aging.

The structure of this thesis begins with an introduction in Chapter 1. Following this introduction, Chapter 2 contains a literature review which summarises description on experimental work reported by various researchers on SAC 305 solder alloy, theory of SPD techniques, UFG materials, ECAP processing, isothermal aging, interfacial IMC formation and mechanism of microstructure evolution during ECAP. Chapter 3 contains the experimental procedure works of the project. Chapter 4 describes on the analysis results and discussion of the project. Conclusions are drawn in Chapter 5.



## CHAPTER 2

### LITERATURE REVIEW

#### 2.1 Solder Alloys

Solder is a process where two metals are metallurgically bonded or joint using solder with a melting point of below 315°C as filler. In other words, soldering can be defined as any types of solder which is being fused and applied in between two metal components in order to attach them together without melting the two metal components. Another definition states that solders are metal alloys that are used to bond or join two or more components. Solders are usually used in holding assemblies, transmitting electrical signals and dissipating heat during service (Ervina and Aisyah 2012).

The bonding action is accomplished by melting the solder material, allowing it to flow among and make contact with the components to be joined, and the components do not melt (Ervina and Aisyah 2012). A chemical reactions between solder and substrate forms intermetallic compounds and this is called bonding process. When molten solder reacts with the solid substrate, two processes are observed to occur simultaneously which are the substrate metal dissolves into the molten metal and the active constituent in the solder combines with the substrate metal to form intermetallic compounds on the surface of the substrate metal (Frear, 1999). The amount of the substrate metal that goes into the solution is related to its solubility in the particular solder and the amount of IMC layer that forms at the surface of the substrate depends more on the solubility of the active element in the base metal. Sufficient thickness of IMC layer is necessary for good wetting but excessive growth of this layer has a detrimental effect to the reliability of the solder joint

since IMC layer is very brittle in nature. Figure 2.1 shows the schematic of solder joint in electronic packaging and Figure 2.2 shows the structure of solder joint and its failure modes.

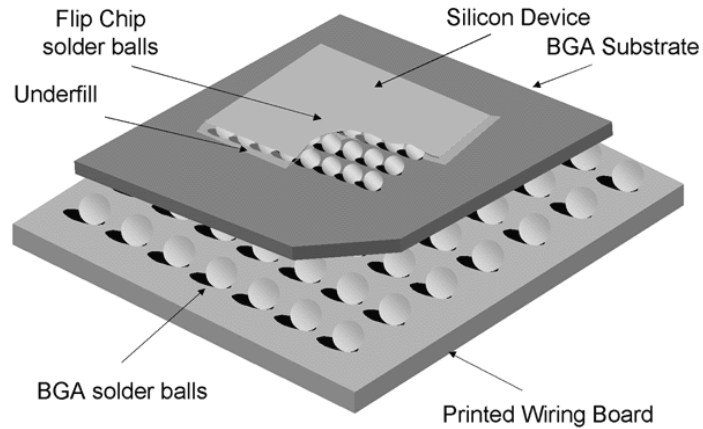


Figure 2.1 Schematic of solder joint in electronic packaging (Frear, 1999)

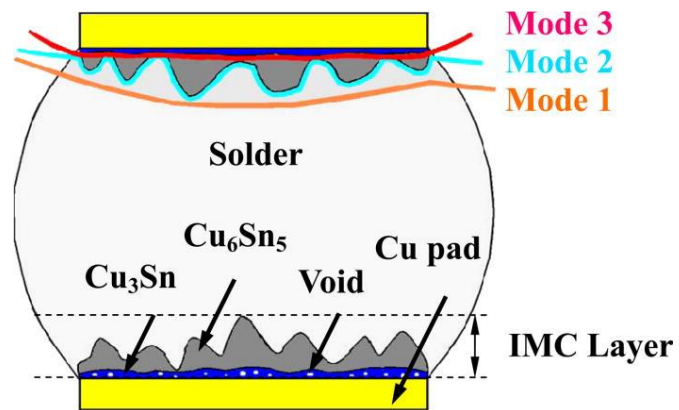


Figure 2.2 Schematic of structure of solder joint and its failure modes (Tong and Fei 2011)

### 2.1.1 Properties of Solder

Solder is a fusible alloy which has lower melting point and excellent wettability. The basic properties of solder that are of importance for electronics application are metallurgical bonding capability with substrate materials, wetting ability during soldering and alloying phenomena between elements alloy (Sriyarunya, et al., 2010). The basic wetting principle during soldering is as shown in Figure 2.3. For a system at a constant temperature T and pressure P, the relationship of surface tension and free energy per area is as below.

$$\left(\frac{\partial G}{\partial A}\right)_{PT} = \gamma \quad (2.1)$$

where G = free energy

A = area

$\gamma$  = surface tension

Then, the thermodynamic condition for spreading to occur is

$$\Delta G < 0 \quad (2.2)$$

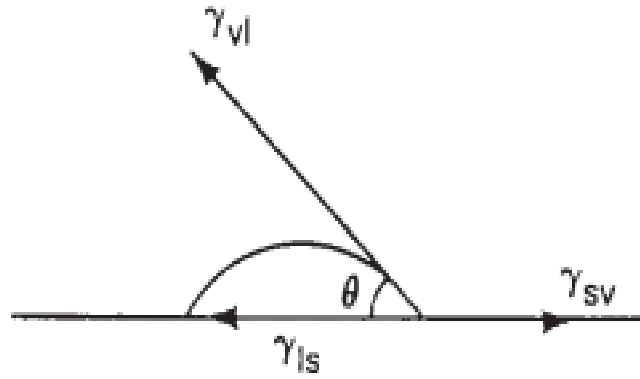


Figure 2.3 Spreading of a liquid with negligible vapor pressure on a solid surface S

(Hwang, 2012)

Thus,

$$-\left(\frac{\partial G}{\partial A}\right)_{P,T} = \gamma_{sv} - (\gamma_{ls} + \gamma_{vl} \cos \theta) \quad (2.3)$$

where  $\gamma_{ls}$ ,  $\gamma_{vl}$ , and  $\gamma_{sv}$  are liquid-solid, liquid-vapor, and solid-vapor interfacial tension, respectively. Thus, for spreading to occur,

$$\gamma_{sv} > \gamma_{ls} + \gamma_{vl} \cos \theta \quad (2.4)$$

### **2.1.2 Sn-Ag-Cu Solder Alloys**

The use of lead-based materials which are usually employed in the electric and electronic industry becomes comprehensive and this has led to a serious problem for environmental and health issues (Vafaenezhad et al. 2016). Therefore, the European directive Restriction of use Hazardous Substances (RoHS) banished the use of lead and other dangerous substances in the electrical and electronic equipments. This restriction drove the need to replace the tin lead (SnPb) solder alloy to lead-free solder alloy where lead (Pb) was banished. In order to replace the tin lead solder, a new alternative solder alloys such as the ternary alloy Sn-Ag-Cu (SAC) in electrical and electronic industry has been made (Berthou et al. 2009) as shown in Table 2.1. Lead free solder is much safer to be used as it is non toxic compared to lead solder. It is also low cost and has comparable mechanical properties with other solders. However, it also has a potential in forming intermetallic (IMC) layer. The nature of IMC layer is usually brittle and can affect the solder joint. In order to prevent from having a brittle solder joint, several solutions have been taken. The researchers have proposed several solutions in solving this problem. Among the potential solutions taken are by adding alloying elements to solder alloy and a severe plastic deformation on solder (Shaeri et al. 2015; Piyavatin et al. 2012) These steps help in improving the mechanical properties of solder alloy.

Table 2.1 : Major lead-free candidates for replacing traditional Sn-Pb solder alloys

(Karl and Kathleen 2004).

Alloy system	Remarks
Sn-Ag	<ul style="list-style-type: none"> <li>• Fairly high melt temperature (221°C)</li> <li>• Alternative for wave soldering but cost an issue</li> <li>• Some reliability concerns related to Ag<sub>3</sub>Sn platelet growth</li> </ul>
Sn-Cu	<ul style="list-style-type: none"> <li>• Fairly high melt temperature (227°C)</li> <li>• Wave solder candidate</li> <li>• Only moderate wetting but sufficient for most applications</li> </ul>
Sn-Zn	<ul style="list-style-type: none"> <li>• Cheap</li> <li>• Lower melt temperature than most Pb-free solders</li> <li>• Zn is highly active, presets potential corrosion and process concerns</li> </ul>
Sn-Ag-Cu	<ul style="list-style-type: none"> <li>• Leading candidate system for reflow soldering</li> <li>• Lower melt point than Sn-Ag, Sn-Cu binary alloys</li> <li>• Adequate wetting, mechanical properties</li> <li>• Much reduced Cu scavenger characteristics compared to Sn-Ag</li> </ul>
Sn-Ag-Bi	<ul style="list-style-type: none"> <li>• Even lower melt temperature than Sn-Ag-Cu</li> <li>• Best fatigue characteristics among most popular Pb-free alloys</li> <li>• Poses some reliability and end-of-life reclamation concerns</li> </ul>

Sn-Ag-Cu solder alloy has many types and was classified according to the composition. For example, SAC 105, SAC 205, SAC 305, SAC 405 and many more. The difference for all of these solder alloy is the composition of Ag. Pb-free SAC alloys range from 1wt% to 5wt% Ag. There are many variations in performance from different SAC alloys as they have different material properties and microstructure. For instances, SAC405 was used as solder balls while SAC 305 was used as solder paste and both of them are slightly similar and can be used together in electronic application. Figure 2.3 shows the phase diagram of SAC alloy.

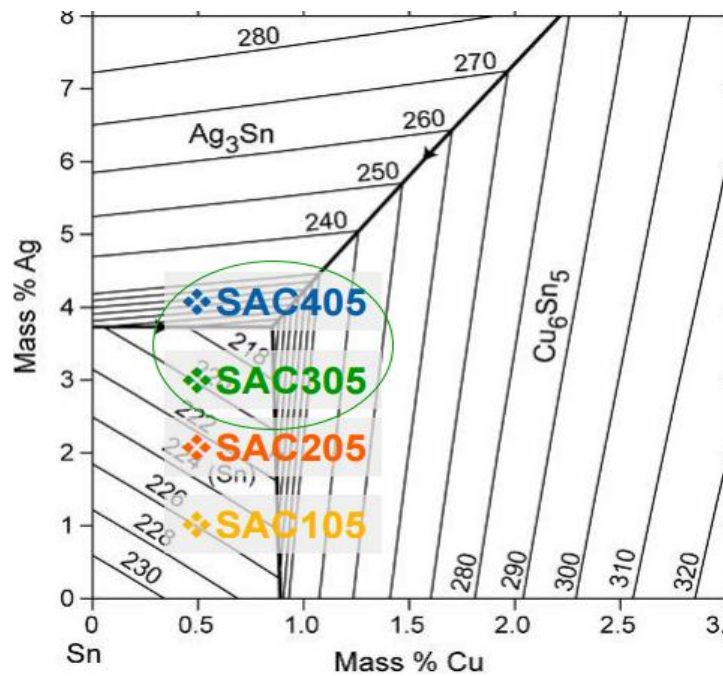


Figure 2.4 Phase diagram of SAC alloy (Moon et al. 2000)

### **2.1.3 Modification in microstructure of Sn-based Solder Alloys**

Modification in microstructure of Sn-based solder alloys can be accessed in many ways. Researchers were trying to find suitable solution in order to improve the properties of this solder alloy. There are several techniques which can be applied to obtain ultra-fine or nano-size grains, e.g. fast solidification, vapour deposition, high-energy ball milling and severe plastic deformation (SPD). One of the methods which is usually used by researchers is by adding alloying elements into compositions of solder alloy such as Ni, Co, Fe, Mn, and Al (Piyavatin et al. 2012). However, certain alloying elements do not give as required properties to solder alloy (Karl and Kathleen 2004). Thus, the modification of microstructure of Sn-based solder alloy accessed by using a severe plastic deformation. The microstructure of Sn-based solder alloys will definitely change when ECAP is applied. ECAP modifies the microstructure of solder alloy from initially coarse grain size to finer grain size (Sanusi et al. 2012). The equal channel angularly pressed (ECAPed) Sn–Ag–Cu alloy was found to exhibit a much greater elongation and lower tensile stress at the low strain rates compared with those of the as-cast alloy (Zhu et al. 2009). Grain refinement of solder alloy achieved from ECAP has been found to improve the mechanical properties of solder alloy.



## **2.2 Theory of Severe Plastic Deformation (SPD) Techniques**

Severe plastic deformation (SPD) is an approach to produce ultra-fined grains through plastically deforming materials to a very large strain which modifies the microstructure of metals including Sn-Ag-Cu solder alloy (Vafaenezhad et al. 2016; Shaeri et al. 2015). By SPD method, the homogeneity of materials increase and produce larger shear strain without changing the cross-section area of the samples. When the pressing is repeated for several passes, samples will likely take a higher shear strain without causing any changes in size or shape and thus, producing an extraordinary grain refinement in which the final angularly pressed solids containing about one thousands or more grains in one segment (Vafaenezhad et al. 2016). A significant grain refinement occurs together with dislocation hardening and precipitation hardening. This mechanism are expected to improve the mechanical properties of materials.

However, SPD technique offers possibility in changing the strain path during deformation besides developing high angle boundaries and granular structures (Verlinden 2009). The SPD technique includes several processes (Figure 2.5), e.g. Equal Channel Angular Pressing (ECAP), High Pressure Torsion (HPT), Accumulative Roll Bonding (ARB), Cyclic extrusion and compression (CEC), Cyclic Close Die Forging (CCDF) and Repetitive Corrugation and Straightening (RCS) (Zrnik et al. 2008; Jain et al. 2014).

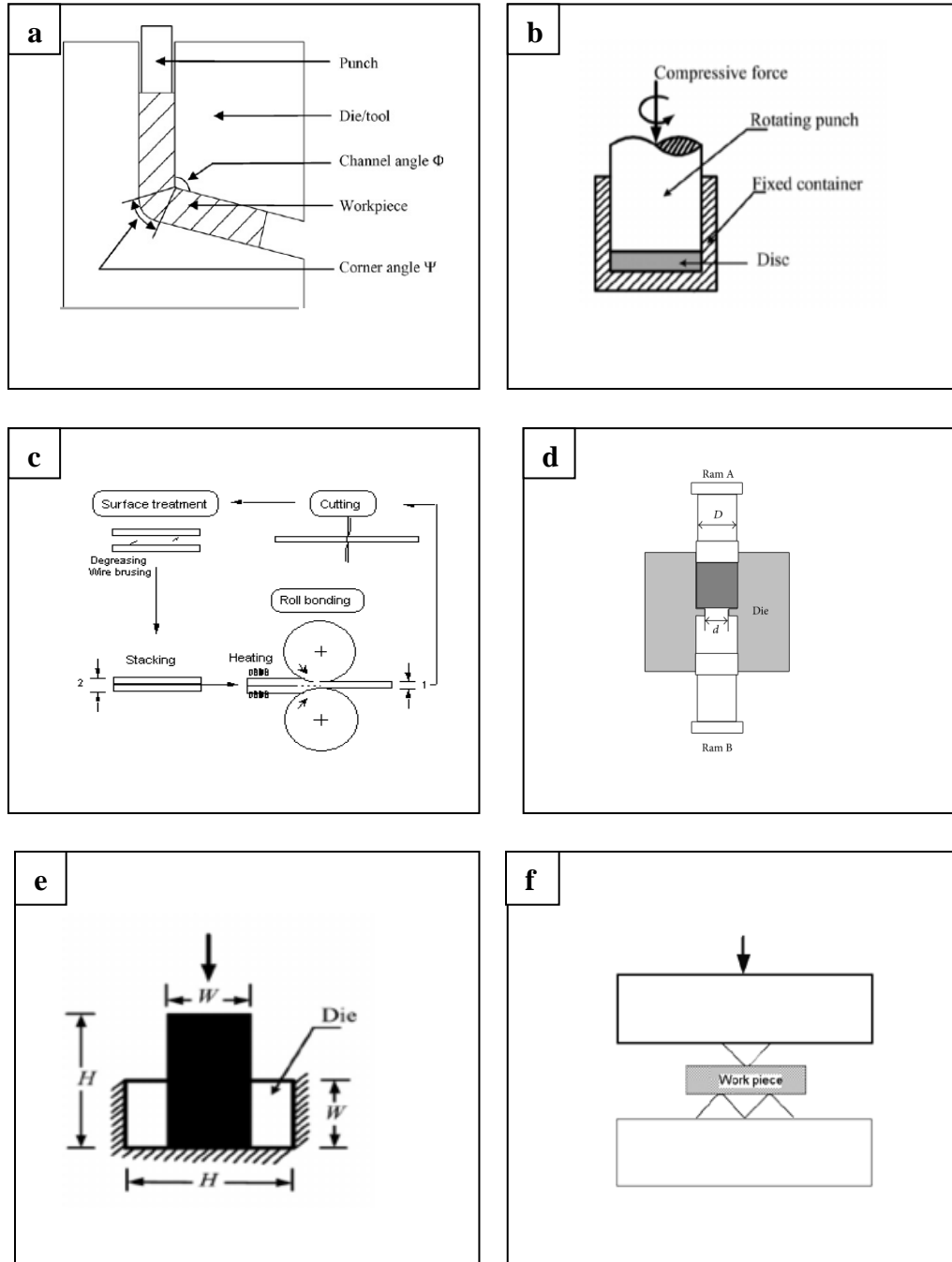


Figure 2.5 Several processes in SPD, (a) Equal Channel Angular Pressing ((b) High Pressure Torsion (HPT) (c) Accumulative Roll Bonding (ARB) (d) Cyclic extrusion and compression (CEC) (e) Cyclic Close Die Forging (CCDF) and (f) Repetitive Corrugation and Straightening (RCS) (Zrník et al. 2008).

ECAP basically involves a pressing of a billet passing through intersecting of two closed channel. After ECAP, the size and shape of the billet remain the same. However, the large amount of redundant deformation in the form of shear takes place, therefore creating ultra-fine grain structure (Jain et al. 2014). In HPT, shear deformation is applied on a material in the form of disk between a fixed die and a rotating punch applying the force in downward direction (Jain et al. 2014). ARB is a method of SPD where two strips of materials are stacked together and passed through counter-rotating rolls. This pressing cause the reduction of 50% as the sheet gets pressed and deformed. The deformed sheet is cut into two pieces, both the pieces are stacked and the process is repeated (Jain et al. 2014). In CEC, a material is extruded by upper ram and reverse extruded by lower ram and finally the extrusion obtain a rod (Lin et al. 2009). In CCDF, a billet of initially height and width is compressed to a certain height and weight. The billet is then rotated by 90° and is compressed again (Jain et al. 2014).

### **2.2.1 Formation of Ultra-fine Grains (UFG)**

Ultrafine-grained (UFG) materials are materials with grain size below 1  $\mu\text{m}$  containing a large fraction of grain boundaries and, therefore, exhibit a wide spectrum of unique properties and property combinations (Leszczyńska-Ma et al. 2016). ECAP produces the very fine grained microstructure of nanostructure by multiple pressings through the die. A research reported that dislocations in grain boundaries were arranged during the development of high angle nano grains in metals and alloys (Zrnik et al. 2008). Severe plastic deformation improved the mechanical properties. The development of

unique superplastic behavior was achieved by the extremely fine grains with high angle boundaries. This is due to the mechanisms of grain boundary sliding or by the grains (Zrnik et al. 2008). Figure 2.6 illustrated the formation of UFG by ECAP before and after ECAP. The grain size of material become smaller after ECAP.

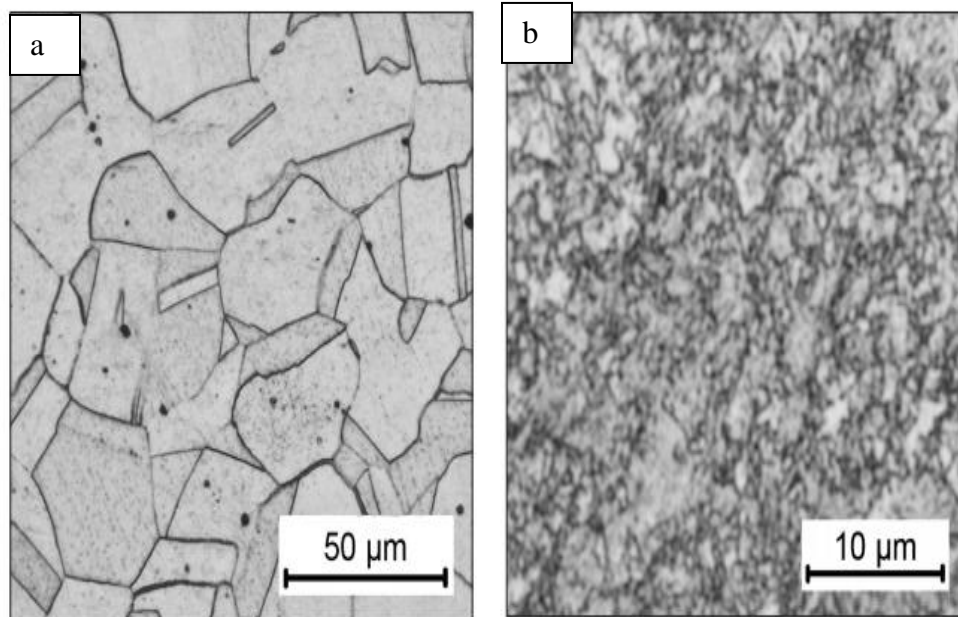


Figure 2.6 The formation of UFG by ECAP (a) before ECAP (b) after ECAP (Zrnik et al. 2008)

### **2.2.2 High Angle Grain Boundaries (HAGB) Improvement in Mechanical Properties via UFG formation**

The grain refinement by ECAP method creates new high angle grain boundaries through three mechanisms. Firstly, during plastic deformation, the grains start to elongate and thus increase the area of high angle boundaries. Secondly, the mechanism of grain

subdivision also allows the creation of high angle boundaries. Thirdly, the elongated grain is split up by a localization phenomenon such as a shear band. From the second mechanism, the grain subdivision starts at low to medium strain when grains break up in cells and cell blocks. The substructures are then changes towards a lamellar structure when strain increases. The new high angle boundaries are then finally generated during this process (Verlinden 2009). Figure 2.7 shows the example of high angle grain boundaries (HAGB) of pure Cu.

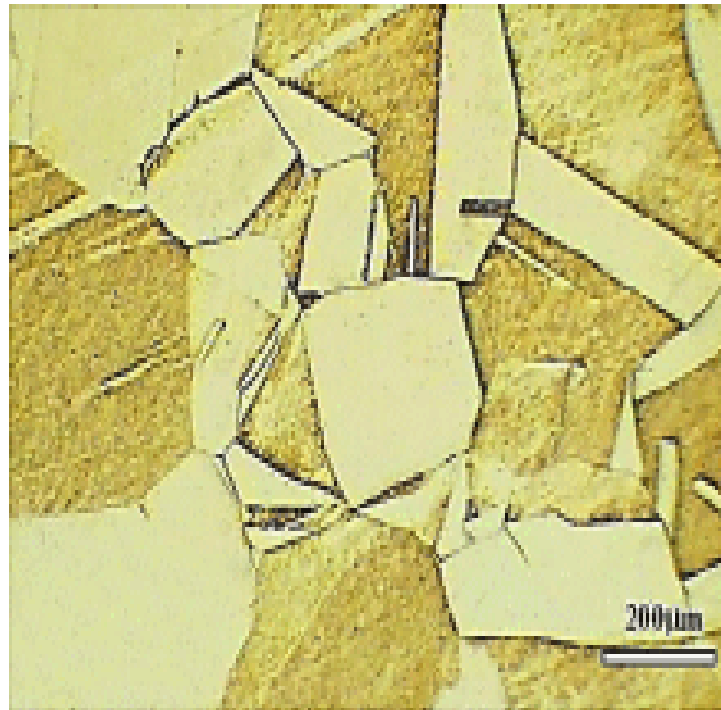


Figure 2.7 High angle grain boundaries (HAGB) of pure Cu (Zhu et al. 2013)

### 2.3 Equal Channel Angular Pressing (ECAP)

Equal channel angular pressing (ECAP) is one of the techniques used to modify microstructure and produce ultrafine-grained (UFG) bulk materials which strongly reduce the grain size of metals and alloys (Figure 2.8). This procedure has the advantage of fabricating fully dense materials without the introduction of any contaminations and large enough for real structural applications (Djavanroodi et al. 2012). The consequence of having a finer grain is providing the potential for superplastic deformation at moderate temperatures and high strain rates. Besides, finer grains are able to significantly increase the strength and fracture toughness of the material (Verlinden 2009). Equal channel angle pressing (ECAP) is also used to alter the microstructure of Sn–Ag–Cu alloy by reducing the large dendrites into fine and equiaxed grains. As the grain boundary area is greatly increased by the ECAP, the alloy should become much more prone to time-dependent deformation.

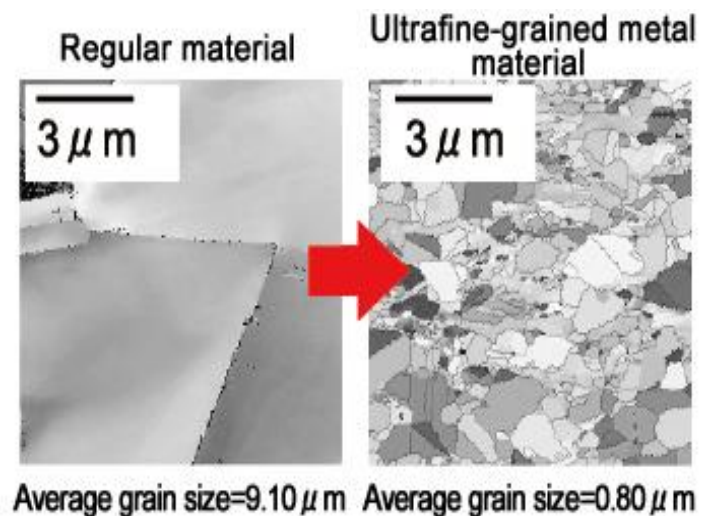


Figure 2.8 Example of microstructure of regular material and ultrafine-grained metal material (Tokushu et al. 2014)

### **2.3.1 Principles of Equal Channel Angular Pressing (ECAP)**

During ECAP, a sample is pressed through two intersecting channels having the same cross-section with a die channel angle and an outer corner angle (Djavanroodi et al. 2012). Since there is no change on the cross-sectional dimension of the specimen during the process, it is now well recognized as a promising method to enhance the strength of various metallic alloys through the occurrence of grain refinement in severe plastic deformation. The intense plastic strain can be achieved by simple shear by pressing the specimen through the two channels.

However, there are several factors which influence the properties and microstructural characteristics of ECAPed SAC solder alloy which are processing route, number of passes, die angle, corner curvature angle and the temperature of the pressing operation (Djavanroodi et al. 2012).

### **2.3.2 Evaluation of strain obtained during ECAP**

ECAP is an SPD process which is most frequently used. ECAP method is basically based on simple shear which taking place in a thin layer at the crossing plane of the equal channels. ECAP becomes the most preferred SPD process because of its low force requirement which requires only small press to press out billet from die tool. The small press also results in low tool pressure and simple tool geometry which is attainable.

However, when ECAP uses low pressure, this maybe causes a problem when processing brittle materials. Brittle materials require slightly higher pressure compared to ductile materials which may require a bit higher pressure to prevent accumulation of damage.

On the other hands, there is still a possibility to process brittle materials in low pressure but the temperature provided must be high enough but still it may changes the behaviour of materials (Zrník et al. 2007)

In ECAP method, the relationship between the strain applied and structure development can be determined. Strain rate determines the constitutive behavior of rate sensitive materials. This is the reason of why it is an important factor in plastic deformation as it determines several behaviours in materials such as dislocation density and flow stress evolution, deformation heat generation.

The strain rate of materials during equal-channel angular pressing (ECAP) was usually evaluated by a geometric approach (Hyoung 2002). Segal has derived an expression for shear strain  $\gamma$  and the process pressure  $p$ .

$$\gamma = \sqrt{3} \frac{p}{Y} \quad (2.5)$$

In this case, friction uniformity in the channels and geometry of channel affect the strain distribution.



The billet is pressed repeatedly for several passes in the same die tool to achieve the required strain. In between each pass, the billet can be rotated about its axis (Zrnik et al. 2007). Figure 2.9 shows the representation of SPD processes in terms of strain distribution

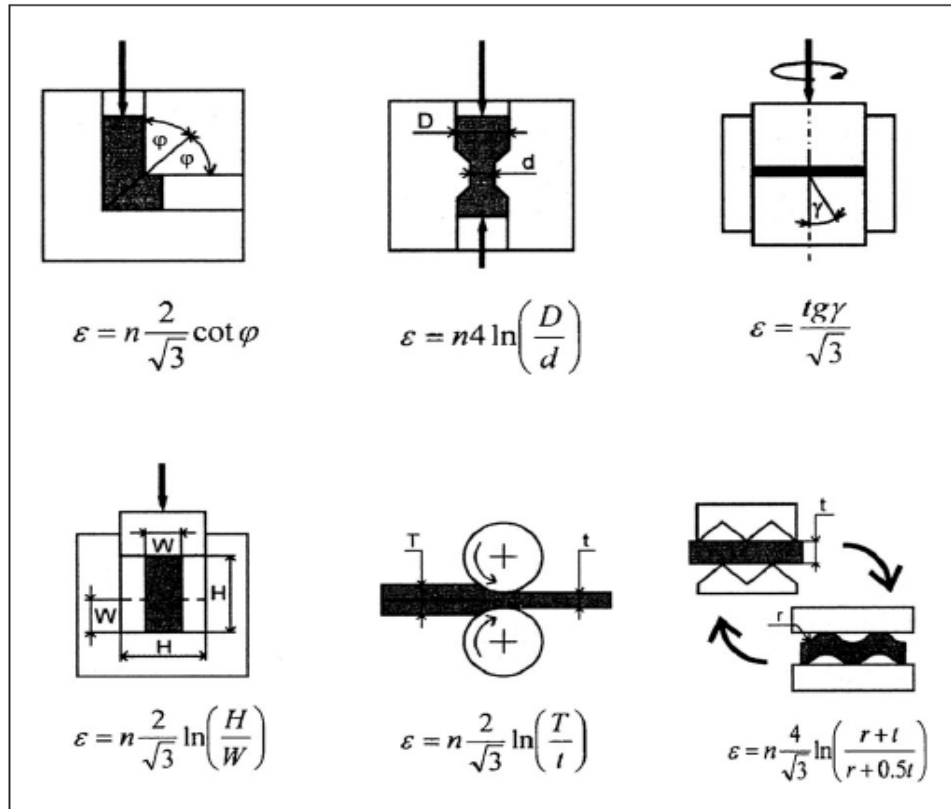


Figure 2.9 Schematic representation of SPD processes in terms of strain distribution (Zrnik et al. 2007).

### 2.3.3 Types of ECAP

Different rotation of billet about its axis will result in different strain in ECAP process. Basically, there are four types of rotations in ECAP which are route A, C, B<sub>A</sub>, B<sub>C</sub> as shown in Figure 2.10 (Zrník et al.2007).

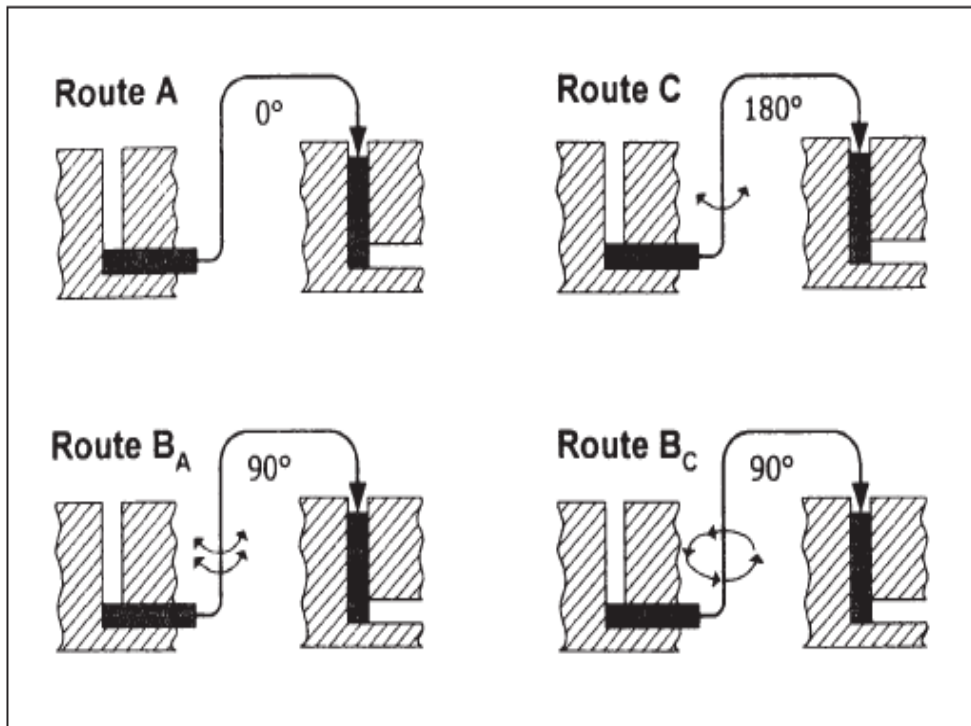


Figure 2.10 Types of billet rotation between consecutive passes through ECAP die tool

(Zrník et al. 2007).

Every route gives different effects of microstructures and properties to the specimen due to the changing of the orientation of specimen between consecutive passes. Route A does not change the orientation of specimen after each pass. Route B rotates the specimen 90°

around its longitudinal axis after each pass. If the rotation is performed in the same direction, it is called route B<sub>A</sub>. The route is called route B<sub>c</sub> if the specimen was rotated alternately between counter clockwise and clockwise. Route C rotates the specimen 180° around its axis after each pass (Kazeem et al. 2012)

#### **2.3.4 Microstructure evolution during ECAP**

ECAP modifies the microstructure of solder alloy into finer grain and forms ultra-fine grain (UFG). During ECAP, microstructure of solder alloy change forms large dendrites into finer dendrites (Zhu et al. 2008).

The distribution of the equiaxed grains microstructure may be due to the deformation of ECAP where the larger shear strain taken place. The finer grain affects the material's behaviour and modification in the mechanical properties of a material.

#### **2.4 Characterization of Solder Materials**

Characterization of solder materials is observed based on several characteristics of solder materials. The characteristics observed from solder materials are its wettability, mechanical properties and IMC layer which forms during reflow and isothermal aging.

### 2.4.1 Wettability

Wettability of solder is determined based on solder's wetting time and wetting angle. One of the factors that governed wetting time is the viscosity of the molten solder; higher viscosity gives longer wetting time. Maximum wetting force is governed by laws of thermodynamics and the surface tension of the solder alloys; higher wetting force indicates lower surface tension and vice versa. The wetting time is in the range if it is below 2 seconds and the wetting angle is below than  $30^\circ$  which are the threshold value for wettability of any solder alloys (Nadhirah et al. 2016). Figure 2.11 shows the schematic of wetting and non wetting solder.

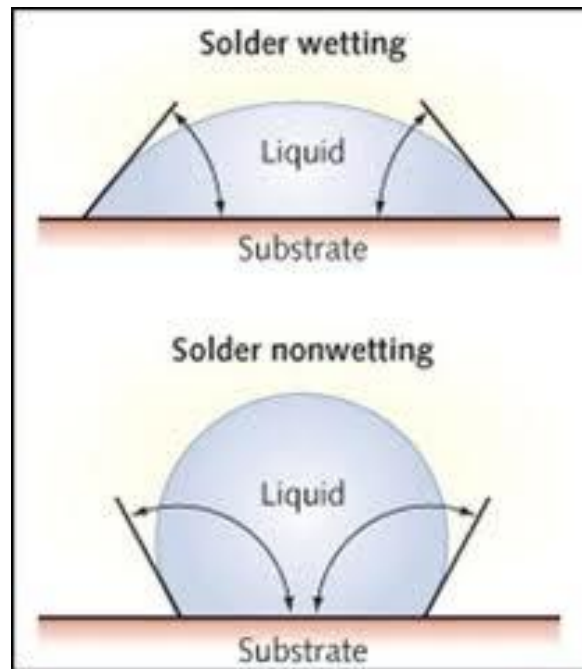


Figure 2.11 Schematic of wetting and non wetting solder (Cup Alloy Ltd. 2017)

In electronic industry, there are several steps that taken into consideration in order to achieve better wettability. The surfaces of substrate should be free of grease and any oxides present before or during the heating cycle in order to allow wetting to occur. The parts should be degreased before soft soldering. Care should be taken not to handle the components in the joint area. Do not use a grit or emery cloth product or scotchbrite for pre-cleaning as they can leave behind deposits that the flux cannot remove and creates pinholes and leaks. The function of the flux is to remove oxide layer. It prepares the surfaces of the parent material to bond with the silver solder. Soft solder fluxes are normally liquid readily applied with a nylon brush. Silver solder fluxes are normally supplied in powder form but are best used as a paste. It is more convenient, easier to use and get good coverage of the joint area. Paste is readily available commercially but can be made in the workshop (Cup Alloy Ltd. 2017)

#### **2.4.2 Mechanical properties of Solder Joint**

Previous studies from Keller et al. (2011) reported that there are several factors which affects the mechanical behaviour of the solder joint (Keller et al. 2011). For instances, the cooling rate, thermal aging, sample size, strain rate or near-eutectic compositional variations. The mechanical behaviour of solder joint depends on the microstructure of the solder and the quality of the intermetallic joining phase. A solder joint should exhibit high strength to withstand high thermal stresses or shock load in order to achieve a long-term reliability. It also should possess adequate ductility in order to absorb sufficient amounts of mechanical energy before cracks and failures are induced (Keller et

al. 2011). Therefore, the microstructure of solder joint should be observed from the beginning stage to the subsequent changes which occur in solder joint. The microstructural changes affects the characteristic lifetime due to solder joints' fatigue. However, the mechanical properties will continuously remain in stable condition if there is only a few changes occur in microstructure of solder joints (Morando et al. 2012).

According to El-Daly et al. (2013), micro-alloying is an effective method to modify the properties of lead-free solder alloys, but adding of these elements also could affect their microstructure and other properties. For this reason, some metal additives, such as Bi, Sb, In, Co, Ga, Ni, Ge and nanoparticles have been introduced into SAC solders to refine the microstructures and reduce the IMC growth.

One of the more noteworthy alloying elements is Ni. It was reported that Ni addition to Sn-3.5Ag in amounts as small as 60.1 wt.% could substantially hinder the  $\text{Cu}_3\text{Sn}$  growth during soldering as well as during the following solid-state aging. A small amount of Ni addition to the Sn–Ag–Cu solders could improve the solder properties, such as the mechanical strength and wettability. Although nickel has a strong influence on solderability and mechanical properties of solders, the detailed mechanism is not fully understood.

Besides, addition of elements such as Sb could improve the mechanical properties, mainly due to the solid solution hardening effects of Sb, formation of the SnSb particles, and the presence of Sb could suppress the coarsening the of  $\beta$ -Sn and refine the  $\text{Ag}_3\text{Sn}$  precipitate, and thus, improve the mechanical and thermal properties of the Sn-based solders (El-Daly et al. 2013).

Another way in improving mechanical properties of solder joint is to applying severe plastic deformation. A research reported on how equal channel angle pressing (ECAP) and was used to alter the microstructure of Sn-Ag-Cu alloy by reducing the large dendrites into fine and equiaxed grains.

As the grain boundary area is greatly increased by the ECAP, the alloy should become much more prone to time-dependent deformation. Thus, it serves as a good model to study how time-dependent deformation behavior may be related to grain boundary in Sn-rich alloys.

As expected, the equal channel angularly pressed (ECAPed) Sn-Ag-Cu alloy was found to exhibit a much greater elongation and lower tensile stress at the low strain rates compared with those of the as-cast alloy. The coarse  $\beta$ -Sn dendritic structure of Sn-3.8Ag-0.7Cu alloy was reduced into a fine equiaxed grain structure by ECAP process. The extruded Sn-Ag-Cu alloy demonstrated quite different deformation behavior compared to the as-cast alloy. ECAP increased the grain boundary volume percentage and the density of grain boundary parallel to the loading direction.

These microstructural changes promoted the time-dependent deformation at low strain rates. The extruded alloy exhibited a much higher tensile elongation but a lower tensile stress at low strain rates compared to the as-cast alloy (Zhu et al. 2009).

### 2.4.3 Intermetallic Compound (IMC) formation

Xiao et al. stated that Sn-Ag-Cu solder alloys exhibit intermetallic structures within the tin-matrix (Xiao et al. 2004). In these intermetallic structures, the compositions present are  $\text{Ag}_3\text{Sn}$  and  $\text{Cu}_6\text{Sn}_5$  (Figure 2.7) (Xiao et al. 2004). A research shows that there are three types of  $\text{Ag}_3\text{Sn}$  compounds which are found to be particle-like, needle-like and plate-like during solidification at different cooling rates. When IMC layer disperse inhomogeneously in Sn matrix, the mechanical properties of solder will be anisotropic (Fei Lin 2011).

Different size of composition presents in solder alloy results in different reliability of solder alloy. For example, defects such as cracks may initiate and propagate along the interfacial between the  $\text{Ag}_3\text{Sn}$  compounds and the solder, if large  $\text{Ag}_3\text{Sn}$  forms at the stress concentration point. Unfortunately, this can damage the reliability of solder joint.

On the other hands, if there is smaller or fine  $\text{Ag}_3\text{Sn}$  precipitates may help to pin the grain boundaries in the solder thus stabilizing the microstructure and strengthen the matrix. Therefore, it is very important to understand the microstructural evolution of these compositions in solder joints especially near the IMC layer during reflow soldering and isothermal aging (Fei Lin 2011).

Figure 2.12 shows the example of IMC layer which composed of  $\text{Ag}_3\text{Sn}$  and  $\text{Cu}_6\text{Sn}_5$  compounds and Figure 2.13 shows thermal fatigue cracks initiate and propagate through intermetallics layer of Sn-Ag-Cu solder.



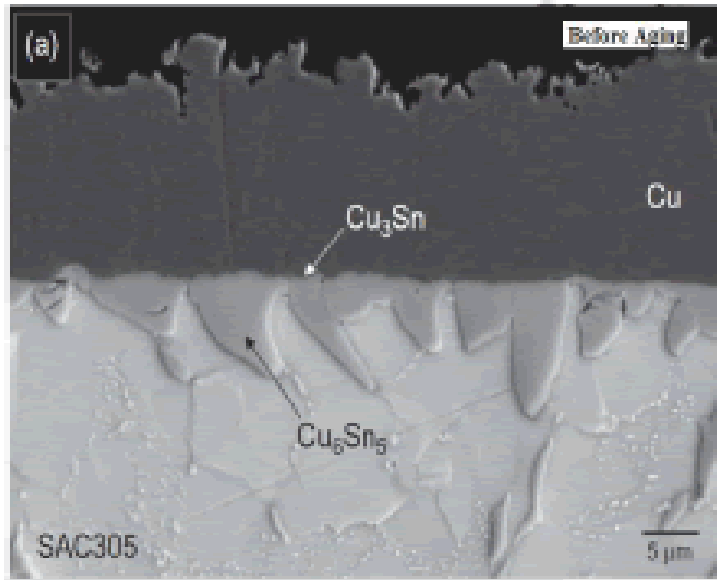


Figure 2.12 Example of IMC layer which composed of  $\text{Ag}_3\text{Sn}$  and  $\text{Cu}_6\text{Sn}_5$  compounds  
(Yasmin et al. 2014)

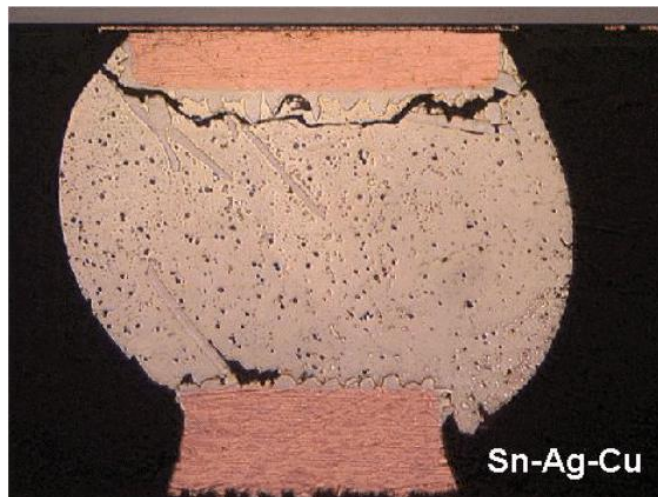


Figure 2.13 Thermal fatigue cracks initiate and propagate through intermetallics layer of  
Sn-Ag-Cu solder (Frear et al. 2001)

In evaluating microstructural changes which occurs in Sn-Ag-Cu solder alloys, aging process is performed to observe the growth kinetics of which formed between solder and substrate (Xiao et al. 2004). During isothermal aging, IMC layer on the substrate can grow due to the reactions which occur between solder and wetting layer (Cu) (Bernasko, 2012). When the solder alloys are isothermally aged, the intermetallics compound layer will grow due to diffusion with thermal energy as its driving force, resulting in much thicker intermetallics compound layer. Diffusion is one of the factors which governed the intermetallics compound layer formation. The previous studies mentioned that IMC layer interfacial growth follows the parabolic growth kinetics (Fick's Law of Diffusion). In brief, the longer the aging time, the thicker IMC layer (Nadhirah et al. 2016).

There is a previous study reported on the effects of addition of alloying elements into lead-free SAC 305 solder paste. Since Sn-Pb provide good mechanical properties compared to Pb-free solder pastes, researchers uniformly reinforced micro-particles (such as Co, Cu, Ag, Ni, and Sb) into the Pb-free solder matrix to form the composite solder, which could increase the reliability of solder joints. While the electronic component getting into miniature in size, reduced in pitch size with demands for high performance application, researchers reinforced the nanoparticles into Pb-free solders to develop high efficiency nanocomposite solders.

Table 2.2 shows the effect of adding various amounts of nanoparticles into a SAC solder paste at solidus and liquidus temperatures.

Table 2.2 Effect of various nanoparticles addition into the lead free solder paste on melting temperature (Chellvarajoo et al. 2015)

Lead free solder paste	Added nanoparticles (wt.% of addition)	Findings			
		Materials	$T_S$ (°C)	$T_L$ (°C)	$\Delta T$ (°C)
Sn-3.5Ag-0.7Cu	TiO <sub>2</sub> (0.5)	SAC	217.3	221.2	3.9
		SAC-0.5TiO <sub>2</sub>	217.7	224.1	6.4
Sn-3.5Ag-0.5Cu	Al <sub>2</sub> O <sub>3</sub> (0.25, 0.5 and 1.0)	SAC	217.7	221.2	3.5
		SAC-0.25Al <sub>2</sub> O <sub>3</sub>	217.4	222.3	4.9
		SAC-0.5 Al <sub>2</sub> O <sub>3</sub>	217.4	222.7	5.3
		SAC-1.0Al <sub>2</sub> O <sub>3</sub>	217.4	223.0	5.6
		SAC	217.0	221.33	4.3
Sn-3.0Ag-0.5Cu	ZrO <sub>2</sub> (0.5, 1.0 and 3.0)	SAC-0.5ZrO <sub>2</sub>	217.08	221.63	4.6
		SAC-1.0ZrO <sub>2</sub>	217.12	221.65	4.5
		SAC-3.0ZrO <sub>2</sub>	217.25	221.95	4.7
		SAC	-	219.9	-
Sn-3.8Ag-0.7Cu	SiC (0.01, 0.05 and 0.2)	SAC-0.01SiC	-	219.2	-
		SAC-0.05SiC	-	219.0	-
		SAC-0.2SiC	-	218.9	-
		SAC	216.31	-	-
Sn-3.8Ag-0.7Cu	Co (0.5, 1.0, 1.5, and 2.0)	SAC-0.5Co	217.68	-	-
		SAC-1.0Co	217.85	-	-
		SAC-1.5Co	217.58	-	-
		SAC-2.0Co	217.70	-	-
		SAC	217.00	221.33	4.3
Sn-3.0Ag-0.5Cu	SrTiO <sub>3</sub> (0.5)	SAC-0.5SrTiO <sub>3</sub>	217.66	221.53	3.9

The results from previous literature revealed that the additions of nanoparticles slightly change the solidus and liquidus temperature from the standard SAC. Overall, the melting range increase with the addition of nanoparticles except the addition of SrTi<sub>3</sub> into the SAC, which reduced its melting range. Therefore, the characteristics of the element in the specific nano powders affect the thermal properties of the particular composite solder

paste. Moreover, the density differences between the elements present in the nanoparticles were varied in the SAC solder paste. Therefore, during the reflow soldering process, there was a high rate of movement in nanoparticles. It might influence the intermetallics (IMCs) layer and cause the reliability issues. The impact of the nanoparticles' mobility was correlated with IMC thickness and mechanical properties of the nanocomposite solder paste. During the reflow soldering process, the solder alloys formed physical bonds with the ferrous elements from the nanoparticles. When the percentage of the nanoparticles was increased in the solder matrix, the newly formed bonds of nano-particles inhibited the entrance of Cu atoms and directly retarded the growth of the IMCs. IMC thickness dropped by after adding  $\text{Fe}_2\text{NiO}_4$  nanoparticles, respectively. The hardness and modulus of the solder microstructure increased with increasing amount of added nanoparticles. However, the optimal amount of added nanoparticles in the Pb-free solder paste is crucial to obtain the optimum efficiency and to minimize the cost of raw materials (Chellvarajoo et al. 2015).

## CHAPTER 3

### MATERIALS AND EXPERIMENTAL PROCEDURES

#### 3.1 Materials and experimental procedures

In this chapter, the materials, ECAP processing, mechanical properties testing, characterization of microstructure and interfacial IMC formation analysis and all experimental procedures involved are explained. The main stages of the study are as follows. Firstly, microstructure of bulk solder alloy and interfacial of IMC formation of solder joint were observed using a Zeiss Supra Gemini 35VP Field Emission SEM (FE-SEM) which is equipped with Energy Dispersive X-ray spectroscopy (EDX). Secondly, the grain size of solder alloy was observed by using I-Solution DT image analyzer software equipped in optical microscope. Thirdly, the hardness of solder alloy is determined by using micro Vickers hardness tester. Lastly, the reflowed and aged solder alloy is then measured with tensile testing by using Instron testing machine. Figure 3.1 illustrates the flowchart of experimental procedures.

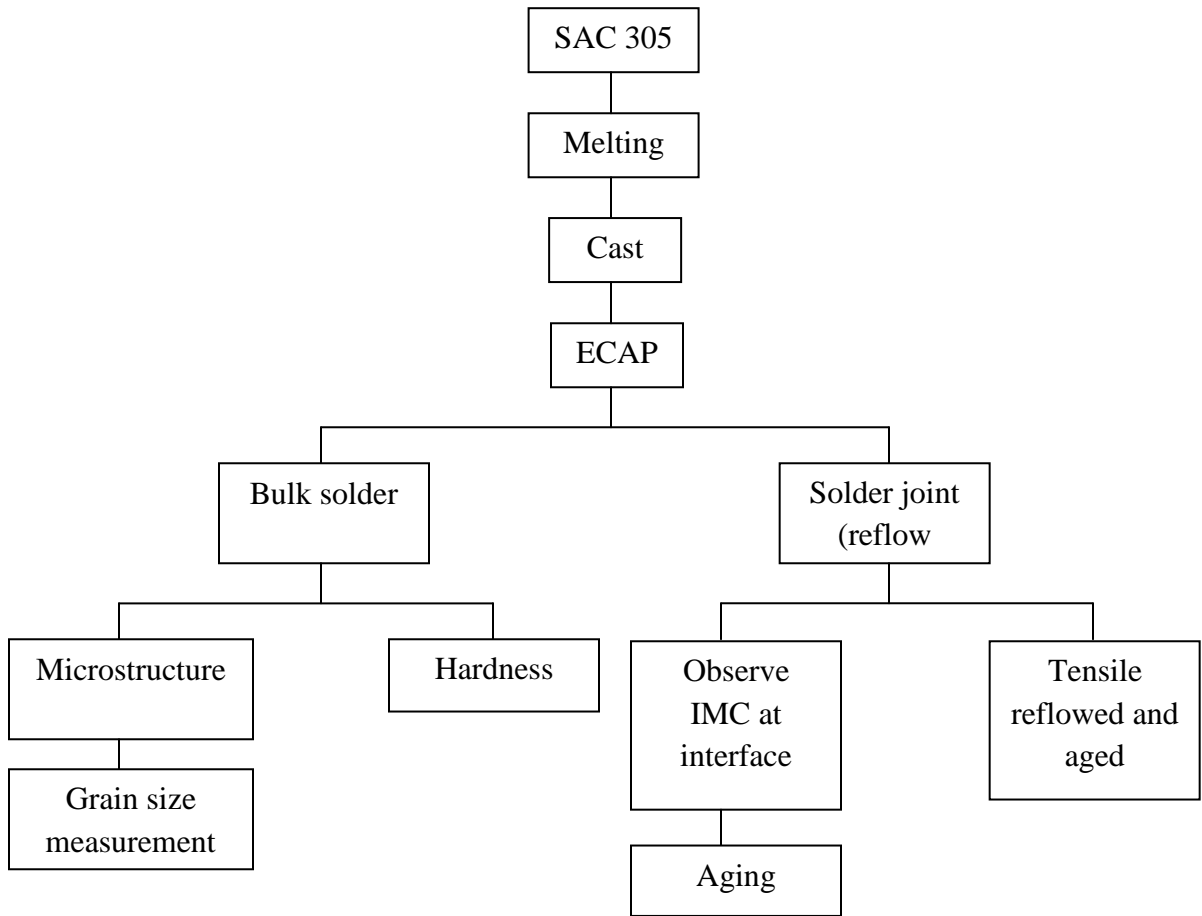


Figure 3.1 Flowchart of experimental procedures.

### 3.2 Materials

Sn-Ag-Cu solder alloy used was commercial solder SAC 305 with composition of Sn-3wt% Ag-0.5wt% Cu. SAC 305 was purchased from RedRing Solder (Malaysia) Sdn Bhd in the form of ingot bar. The chemical composition of SAC 305 is as shown in Table 3.1. The bar was rectangular in shape with 375 mm long, 20.0 mm width and 8 mm thickness.

Prior to ECAP process, the solder bar need to be remelted and cast into cylindrical shape to be fed into the ECAP mold. The bar was cut and weighed for 90 g to be melted inside a graphite crucible in a box furnace at 350°C. The heating rate of the furnace was set to be 10°C/min. The molten solder was stirred every hour to ensure homogeneity of the alloy. The soaking time was set to be 2 hrs.

The heating profile is as shown in Figure 3.2. The solder alloy was then cast into cylindrical billet in a mild steel mold.

Table 3.1 Chemical composition of SAC 305 solder alloy

<b>Element</b>	<b>Weight percentage (%)</b>
Sn	96.44
Pb	0.034
Cu	0.495
Ag	2.980

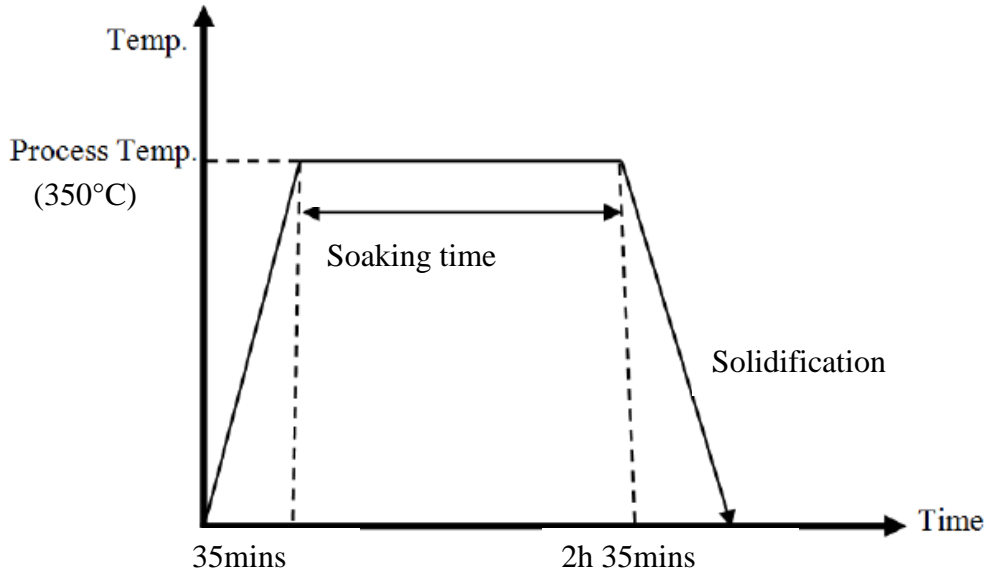


Figure 3.2 Heating profile of SAC solder alloy

### 3.3 ECAP processing

The SAC 305 solder was in the form of cylindrical rod after casting. During the ECAP processing, the cylindrical billet with length of 6.5 mm and diameter of 1.9 mm was inserted into an ECAP die made of tool steel. A plunger was inserted into the die to force the sample through the die. The samples were forced through an ECAP pressing die of two channels which intersect at an angle of  $120^\circ$  which is known as die angle ( $\Phi$ ) shown in Figure 3.3. Each billet was pressed with different number of passes of 0, 4 and 9 passes and was not rotated with respect to the longitudinal axis in the same direction between the two consecutive passes as shown in Figure 3.4. This route was designated as route A (Zhu & Lowe 2000). Figure 2.3 shows the route Bc of ECAP where the billet being rotated into  $90^\circ$  with respect to the longitudinal axis. The die has a curvature angle ( $\psi$ ) of  $20^\circ$ .



The pressing was applied by UTM (Universal Testing Machine) with pressure of 500 MPa to 900 MPa depending on the number of passes. The pressed rods were inserted back into the ECAP die for consecutive pressings. Before pressing, the billets were lubricated with MoS<sub>2</sub> lubricant to reduce the friction between the plunger, billets and the die wall. The plunger was aligned carefully through the upper channel of the die in order to avoid the plunger from bending.

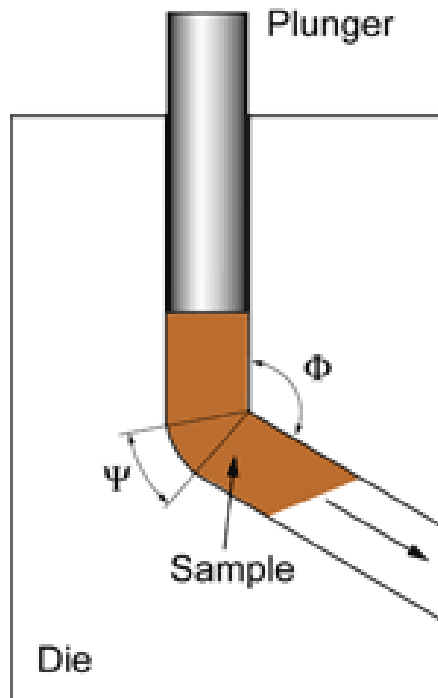


Figure 3.3 Processing of equal channel angular pressing (ECAP) (Furukawa et al. 2001)

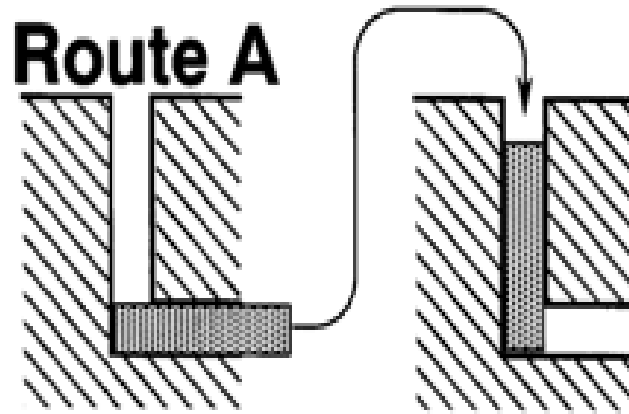


Figure 3.4 Route A in ECAP processing (Shanon et al. 2015)

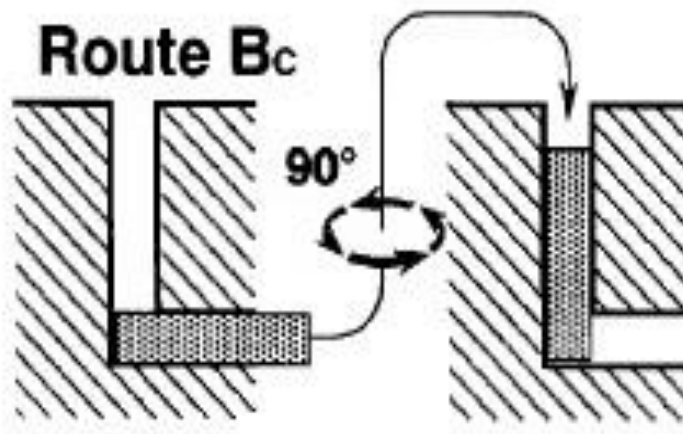


Figure 3.5 Route Bc in ECAP processing (Shanon et al. 2015)

### 3.4 Reflow process

Prior to isothermal aging, the sample was reflowed first. The sample was cut from ECAP rods to form solder disc with a thickness of 0.5 mm. The solder disc was then ground using SiC paper grit 800 and 1000 in order to remove contaminants on the surface of the disc. After grinding, the solder disc was punched into a smaller disc of 6 mm diameter. The solder disc was then placed on Cu substrate which was cut into 1.5 mm x 1.5 mm in dimension and the thickness was 0.5 mm. The Cu substrate was previously ground in order to remove any oxide layer. Before the sample was placed on the Cu substrate, activated rosin (RA) flux was applied to the surface of the substrate to remove any oxide layer and other contaminants. The reflow process was performed at 260°C for 10 s in a reflow oven. Figure 3.6 illustrates the schematic of reflowed solder sheet embedded on Cu substrate.

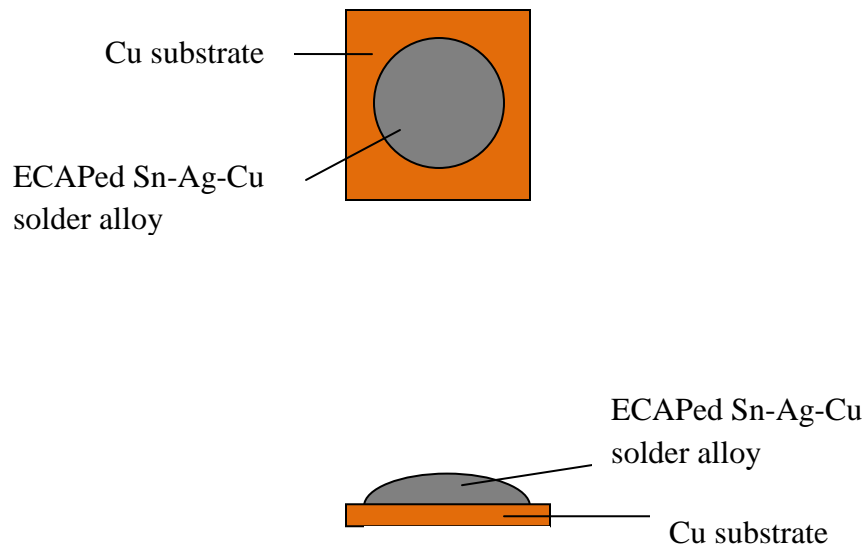


Figure 3.6 Reflowed solder sheet embedded on Cu substrate

### **3.5 Isothermal aging**

After reflow, the sample was isothermally aged at 180°C for different periods of time in an aging oven with model namely Memmert Muffle. The aging time was set for 100 hours, 250 hours and 500 hours.

### **3.6 Mechanical properties testing**

Mechanical properties assessed in this work are microhardness testing and tensile testing.

#### **3.6.1 Microhardness testing**

Before microhardness testing, the cylindrical ECAP processed rod was sectioned perpendicular to their longitudinal axes. The rod was cut into a thickness of 2 mm. The circular surface of rod was ground by sand papers from 800 grits to 2000 grits and then polished to a mirror-like finish. Microhardness testing was carried out on a micro Vickers hardness tester. Each sample was indented in centre area under a load of 5 kgf and 15 s dwell time. All microhardness data of different number of passes were taken as the average of at least three indentations. Figure 3.7 shows schematic representation of Vickers hardness indentation.

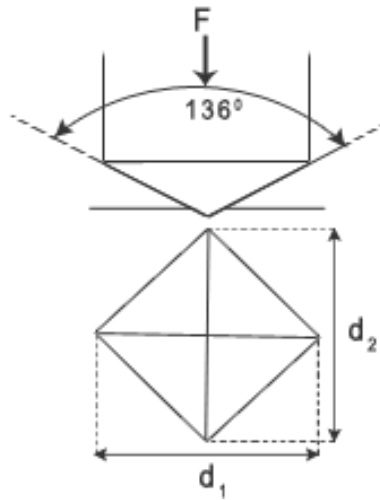


Figure 3.7 Schematic representation of Vickers hardness indentation (Hiox India, 2017)

### 3.6.2 Tensile testing

Tensile testing was performed in order to investigate the deformation of behaviour of the ECAPed alloy. The tensile test was performed by using an Instron type testing machine at room temperature. Tensile test sample was cut from the cylindrical ECAP processed rod and ground by sand paper from 800 grits to 1000 grits. After grinding, the thin cylindrical ECAPed alloy was cut with cross-section of 3.0 mm x 3.0 mm dimension. This sample was then placed on copper substrate of 15 mm x 15 mm dimension before reflowed. After reflowed, tensile test was performed on the sample. Figure 3.8 shows the sample prepared for lap joint tensile strength test. The test was carried out using an Instron testing facility.

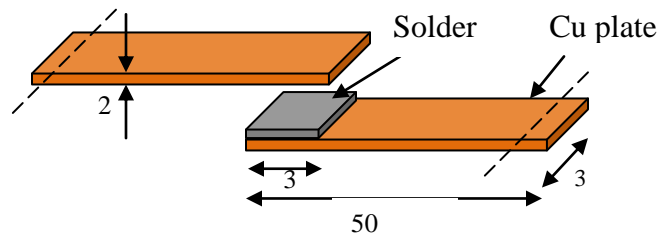


Figure 3.8 Lap joint for shear test

### 3.7 Characterization

The characterization of bulk solder and interfacial IMC layer at interface were investigated by using Scanning Electron Microscopy (SEM), X-ray Fluorescence (XRF), Optical Microscopy (OM), Stereo Zoom Microscope.

#### 3.7.1 Scanning Electron Microscopy

Scanning electron microscopy (SEM) is usually used to analyse surface topographic. A Zeiss Supra Gemini 35VP Field Emission SEM (FE-SEM) which is equipped with Energy Dispersive X-ray spectroscopy (EDX) was used to observe bulk microstructure of samples and interfacial IMC at the solder joint. The bulk solder sample was ground with SiC paper grit 800 to 2000 and polished with 9  $\mu\text{m}$  diamond media, 3  $\mu\text{m}$  diamond media and colloidal silica. Then, the sample was cleaned in an ultrasonic bath and finally etched with 5ml  $\text{HNO}_3$ -2ml  $\text{HCl}$ -93ml  $\text{H}_2\text{O}$  etching solution to reveal the microstructure. On the other hand, the reflowed sample which used to observe IMC layer was also prepared to reveal interfacial IMC at the solder joint.

### 3.7.2 X-ray Fluorescence

X-ray Fluorescence is used to determine the composition of elements that present in material. The elements assumed to present in the bulk solder alloy were Sn, Ag and Cu. XRF analyzers measure the secondary X-ray emitted from a sample when it is excited by a primary X-ray source as to determine the chemistry of a sample.

### 3.7.3 Optical microscopy

The reflowed solder was cross-sectioned, mounted and ground using SiC paper grit 800 to 2000. Then, the sample was polished with 9  $\mu\text{m}$  diamond finish paste, 3  $\mu\text{m}$  diamond finish paste and silica to reveal the cross section of the solder joint. As the sample was prepared, the wetting angle was measured from the cross-sectioned sample by using I-Solution DT image analyzer software equipped in optical microscope. Besides, the average grain size was also measured by using this software which equipped in optical microscope. The average thickness of the total IMC layer was measured by quantitative image analysis. As illustrated in Figure 3.9, the area A of the IMC layer, the hatched area was measured and then was divided by the layer length L to obtain the average thickness.

$$\text{Average IMC thickness} = \frac{A}{L} \quad (3.1)$$

where

$A$  = Area of the IMC layer

$L$  = Length of IMC layer

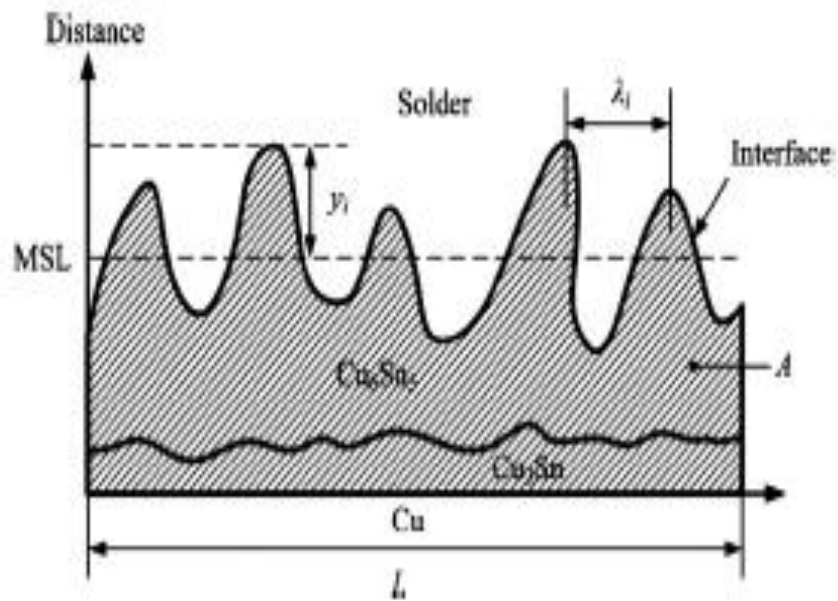


Figure 3.9 Definition of the parameters to characterize the IMC microstructure (Tong et al. 2014)

### 3.7.4 Stereo Zoom Microscope

A spreading test was carried out to measure the diameter of the solder alloy and observe how it spread on Cu substrate.



The diameter of solder alloy was measured by using Stereo Zoom Microscope Kunoh Robo. After reflow, the sample underwent spreading test to observe the spreading of the solder alloy. Figure 3.10 shows the stereo zoom microscope and Figure 3.11 shows the measurement of diameter of reflowed solder.

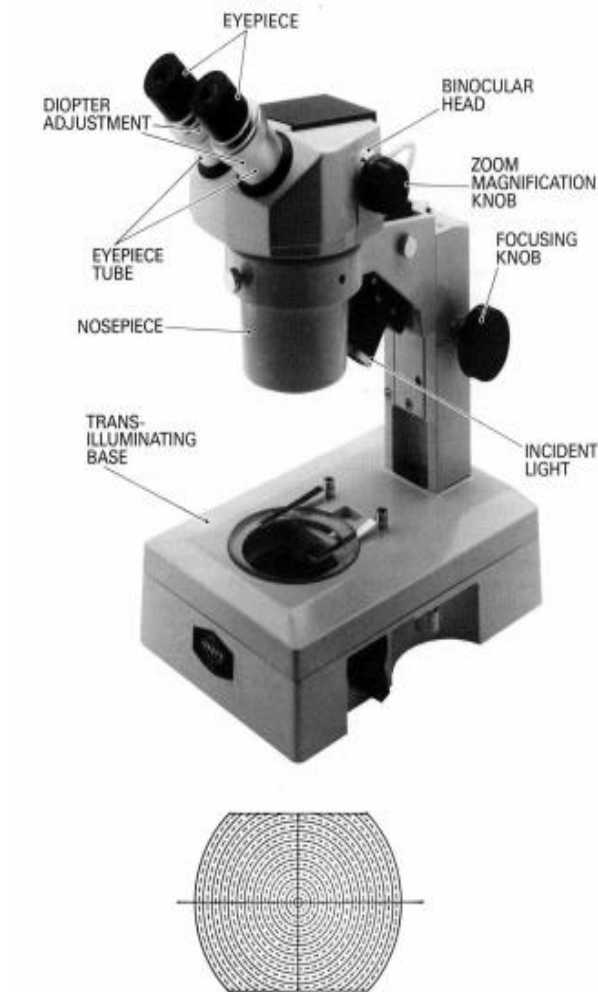


Figure 3.10 Stereo Zoom Microscope (Swift,1990)

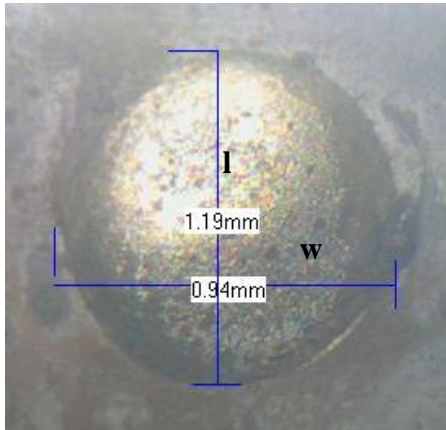


Figure 3.11 Measurement of diameter of reflowed solder on Cu substrate

## CHAPTER 4

### RESULTS AND DISCUSSION

#### 4.1 Overview

This work analyses on how a severe plastic deformation of ECAP influences the properties of solder alloy. It has been generally known that ECAP modifies the microstructure of solder alloy by refining the grain size and creates ultra-fine grain (UFG). As significant grain refinement occur, the mechanical properties of solder are expected to be improved. The finer the grain produced by ECAP, the higher the mechanical properties of solder alloy and thus could improve the reliability of solder joint.

#### 4.2 Microstructure evolution of Sn-Ag-Cu solder alloy

Microstructure evolution of the solder alloy involves microstructure of bulk ECAPed solder alloy and grain size measurement of the solder. Observation of solder microstructure following ECAP process would enable better understanding on the influence towards mechanical properties and IMC behaviour during aging.

##### 4.2.1 Microstructure of bulk ECAPed solder alloy

Figure 4.1 shows the microstructure of Sn-Ag-Cu bulk solder alloy with different number of ECAP passes. The microstructure of 0 pass solder alloy features typical phases observed in SAC alloy, as labelled in Figure 4.1. Large  $\beta$ -Sn dendrites were observed to be

the light areas. Eutectic networks surrounds the  $\beta$ -Sn dendrites. These eutectic regions consisted of  $\text{Ag}_3\text{Sn}$  and  $\text{Cu}_6\text{Sn}_5$  precipitates and the Sn matrix (Tabassum et al. 2014). From Figure 4(a) to (c), it can be seen that the bulk microstructure changes from 0 pass to 9 passes. It can be observed that the  $\beta$ -Sn dendrites seem to be elongated and thinner when the number of passes applied on solder alloy was higher. This is due to the deformation in solder alloy which occur by route A of ECAP. Djavanroodi et al. (2012) illustrated that route A causes strain deformation but the strain is the lowest among other routes of ECAP (Djavanroodi et al. 2012). Route A produces a decrease in strain distribution uniformity with increasing ECAP pass number and this is why the  $\beta$ -Sn dendrites elongated and thinner. The dendrites may become thinner but not in a uniform shape grain due to the lowest strain produced by route A. It is also apparent that the eutectic network was more evenly distributed along the elongated  $\beta$ -Sn grains.

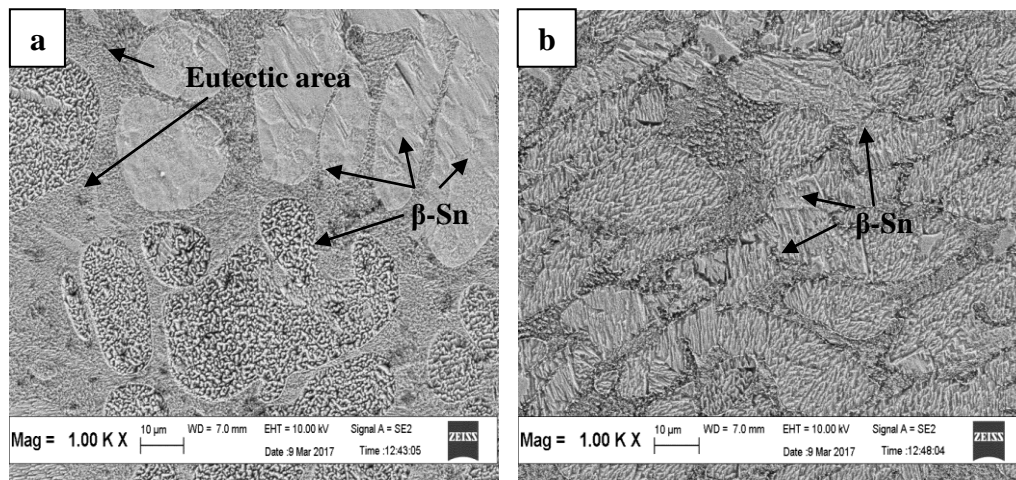


Figure 4.1 SEM microstructure of ECAPed solder alloy with (a) 0 pass (b) 4 passes and (c) 9 passes

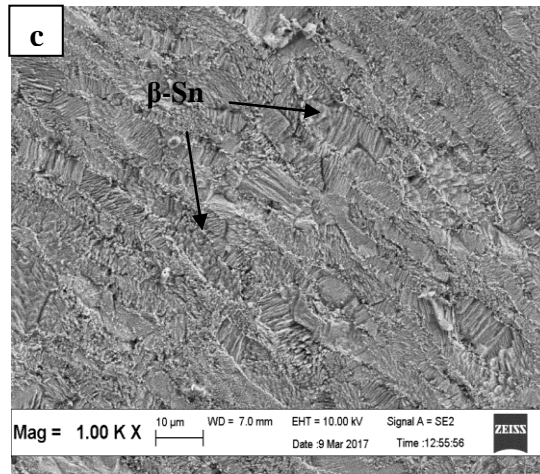


Figure 4.1 (continue)

#### 4.2.2 Grain size measurement

Figure 4.2 shows the scanning electron microscopy images of grain size measurement of solder alloy on which the grains were measured with different number of ECAP passes. From the figure, it could be seen that the grain sizes were finer as the number of passes increased. Grain sizes of 9 passes were significantly finer compared to that of for 0 pass. Zrnik et al. (2007) reported that this severe plastic deformation (SPD) technique produces finer subgrains in the initially coarse grain material (Zrnik et. al 2007). The grain refinement is likely to occur due to short and long-range intersecting shear bands produced by plastic deformation which occur at grain subdivision and local dynamic recovery process. However, there is a study which stated that the grain refinement occur because of recrystallization process. Due to the low melting temperature of the solder alloy, a recrystallization may very well occurred during ECAP pressing.

$$\text{Recrystallization } T = 0.3T_m \quad (4.1)$$

$T_m$  of solder = 217°C

So,

$$\text{Recrystallization } T = 0.3 (217)$$

$$= 65.1^\circ\text{C}$$

where

$T$  = Temperature

$T_m$  = Melting temperature

There is a probability that recrystallization occurred and thus, contributed to the grain refinement (Zhu et al. 2008).

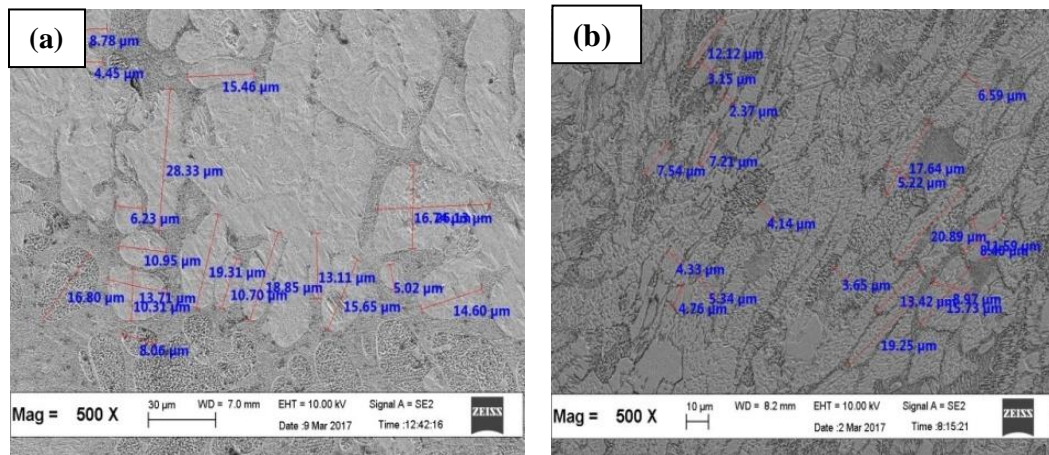


Figure 4.2 Scanning electron microscopy images used in the measurement of grain size of solder alloy with different number of ECAP passes (a) 0 pass (b) 4 passes and (c) 9 passes

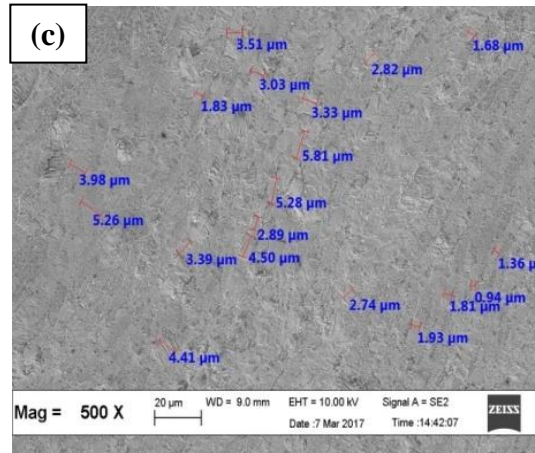


Figure 4.2 (continue)

Table 4.1 lists the average grain size for ECAPed solder at 0, 4 and 9 passes. It can be seen that the grains size for 0 pass is 13.07  $\mu\text{m}$ , which is the largest among the samples. The grain size decreased when the number of pass increased. As the number of pass increased, more deformation and higher strain experienced by the solder, creating refinement of grains. The result agreed well with other researchers working on ECAP of various metals.

Table 4.1 Average grain size of solder alloy after ECAP pressing

Variable	Average grain size ( $\mu\text{m}$ )		
	0 pass	4 passes	9 passes
Minimum	4.45	2.37	0.94
Maximum	28.33	20.89	5.81
Mean	13.07	8.83	3.27
Standard deviation	7.13	6.37	1.68

### **4.2.3 Comparison of microstructure of ECAPed bulk solder alloy with different routes**

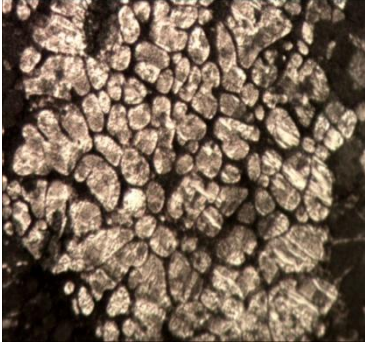
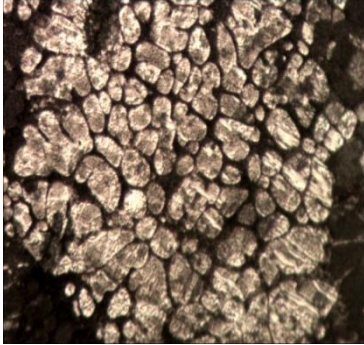
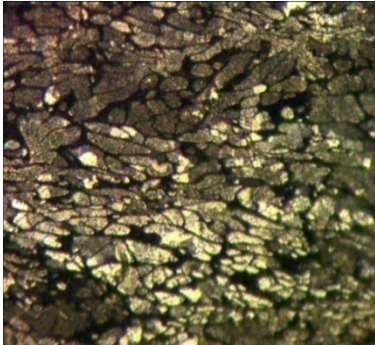
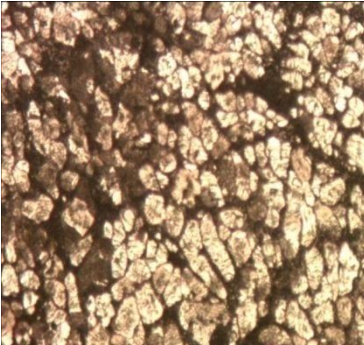
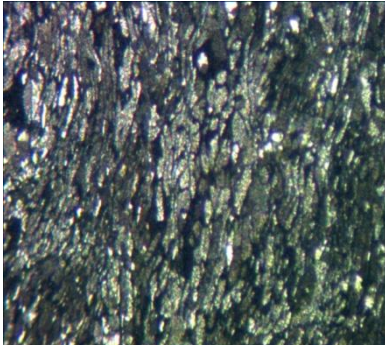
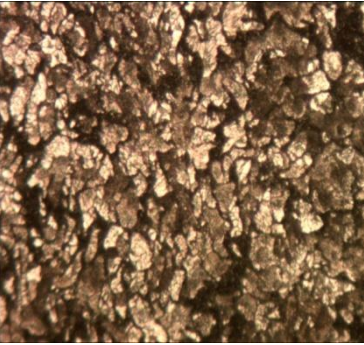
Table 4.2 shows the microstructure of ECAPed bulk solder alloy with routes A and route B<sub>c</sub>. The microstructure of bulk ECAPed solder alloy with route A and route B<sub>c</sub> are slightly different.

This can be observed in microstructure of bulk ECAPed solder alloy with 9 passes for both routes. The grains in sample of 9 passes of route A is significantly elongated and thinner whereas the grains in sample of 9 passes of route B<sub>c</sub> is rounder in shape and more uniform. This result is in agreement with other reported works in which they have stated that route B<sub>c</sub> produced uniform distribution of finer grain size compared to route A (Kazeem et al. 2012).

Besides, this result is affected by the nature of route itself. Route A does not change the orientation of specimen after each pass whereas route B<sub>c</sub> rotates the specimen 90° around its longitudinal axis after each pass alternately between counter clockwise and clockwise (Zrnik et al. 2007). The rotation enable deformation to occur in different plane orientation creating an equiaxed grains compared to that of produced via route A.



Table 4.2 Optical microscopy images of bulk ECAPed solder alloy of route A and route Bc  
0 pass, 4 passes and 9 passes

Number of passes	Route A	Route Bc
0 pass		
4 passes		
9 passes		

### 4.3 Wettability of reflowed ECAPed Sn-Ag-Cu solder alloy

Table 4.3 summarizes the wetting angles of ECAPed solder alloy after reflow. Generally, the wetting angle of samples from three different number of passes were slightly different among each other. The average of wetting angles was achieved from wetting angle of 3 samples. 0 pass sample displayed higher wetting angles compared to 9 passes. However, the wetting angles were still in the range below than 30° which are the threshold value for wettability of any solder alloys (Nadhirah et al. 2016).

Table 4.3 Wetting angles of ECAPed solder alloys (°)

Specimen	Sample			
	1	2	3	Average
0 pass	26.38	25.86	27.05	26.43
4 passes	25.30	25.26	25.70	25.42
9 passes	24.75	25.48	25.55	25.26

### 4.4 Spreading test

Table 4.4 below shows the spreading test of ECAPed Sn-Ag-Cu solder alloy with different number of pass after reflowed on Cu substrate. The diameter of the three samples of different passes is slightly similar as shown in Table 4.5. The diameter of the three samples

of different passes is slightly similar because when the solder melts, the strain induced by ECAP was still remain and the grain still same.

Table 4.4 Spreading test of ECAPed Sn-Ag-Cu solder alloy reflowed on Cu substrate with 0 pass, 4 passes and 9 passes

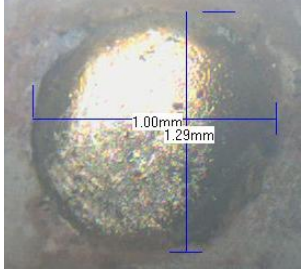
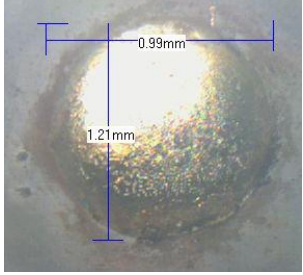

Number of passes	Diameter measurement
0 pass	
4 passes	
9 passes	

Table 4.5 Length and width of reflowed solder on Cu substrate

Specimen	Length (mm)	Width (mm)
0 pass	1.00	1.29
4 passes	0.99	1.21
9 passes	0.94	1.19

#### 4.5 Microhardness of ECAPed solder alloy

The results of Vickers hardness test for Sn-Ag-Cu solder alloy during ECAP process with different number of passes are as shown in Table 4.6 and Table 4.7. By using 1 kgf load, it could be observed that the solder alloy which underwent 9 passes had the highest hardness value compared to solder alloy with 0 pass which had the lowest hardness value. As the number of ECAP passes increased, the hardness of solder alloy increased. By comparing with microstructure of bulk solder and grain size of the solder, the hardness of solder follows the Hall-Petch relationship where a finer grain would give higher hardness.

The 9 passes solder which possess the highest hardness has a finer grain size among others. This shows that the finer grain which produced by ECAP has increase the hardness of solder. The observation obeyed the Hall-Petch relationship where hardness increases upon decreasing grain size. The Hall-Petch relationship describes how the yield stress of a polycrystalline material increases when its grain size decreases.

The relation is based on the dislocation mechanism of plastic deformations as the formation of grain boundaries could hinder the movement of dislocations. When the grain sizes decreases, more grain boundaries is formed and thus hinder the dislocation movement. This makes the material harder and stronger. A study reported that grain boundaries and their underlying structure are known to play an important role in the bulk properties of polycrystalline materials. Moreover, grain boundaries have an increased role in determining the functional and mechanical properties of nanocrystalline materials as the grain size decreases to nanoscale dimensions (Tschopp and McDowell 2008).

However, when comparing both route A and route B<sub>c</sub> as shown in Figure 4.6, route B<sub>c</sub> shows higher hardness compared to route A. This is because the grain produced by route B<sub>c</sub> is slightly finer compared to route A as illustrated before in Figure 4.4 and Figure 4.5. Therefore, it is significant that route B<sub>c</sub> creates a better improvement of mechanical properties of solder alloy compared to route A as the finer the grain size produced, the higher the hardness achieved.

Table 4.6 Vickers hardness reading (Hv) for route A

Specimen	Sample			
	1	2	3	Average
0 pass	14.5	14.5	14.6	14.5
4 passes	14.9	14.8	14.8	14.8
9 passes	15.3	15.2	15.3	15.3

Table 4.7 Vickers hardness reading (Hv) for route B<sub>c</sub>

Specimen	Sample			
	1	2	3	Average
0 pass	14.5	14.5	14.6	14.5
4 passes	14.8	15.3	15.1	15.1
9 passes	15.5	15.7	15.8	15.7

#### 4.6 Isothermal aging

Figure 4.3, Figure 4.4, Figure 4.5 and Figure 4.6 show the microstructure of IMC layer of solder alloy of route A with different ECAP passes of 0 pass, 4 pass and 9 passes at solder-substrate interface for reflowed and after isothermally aged at 180°C for 100, 250 and 500 hours respectively. Table 4.8 lists the thickness of IMC layer for all different ECAP passes of solder alloys for reflow and isothermal aging at 180°C for 100 hours, 250 hours and 500 hours. Reflow sample of 9 ECAP passes showed the thinnest IMC layer followed by 4 passes and 0 pass which gave the thickest IMC layer. The higher number of ECAP passes results in reduction of thickness of interfacial IMC layer. It is possible that the diffusion of active species during reflow was slowed down by the re-distribution of eutectic network following ECAP. As can be seen from Figure 4.1 (b) and (c), the eutectic network has been re-arranged as the solder deformed. Thus, the arranged network of IMC particles could become barrier to slow down diffusion.

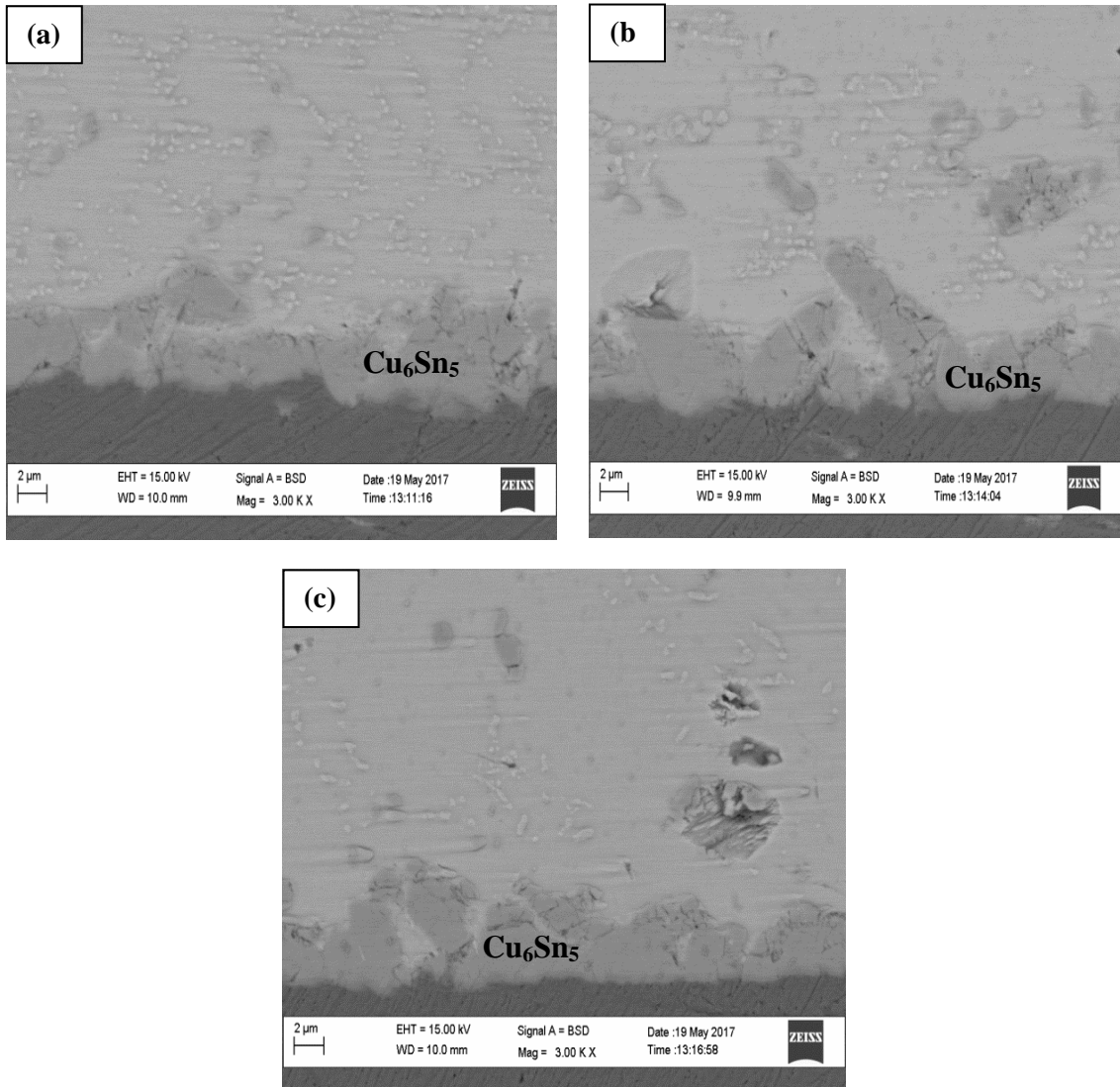


Figure 4.3 IMC layer at solder-substrate interface for reflowed samples of route A ECAP,  
(a) 0 pass (b) 4 passes and (c) 9 passes ECAPed solder alloys

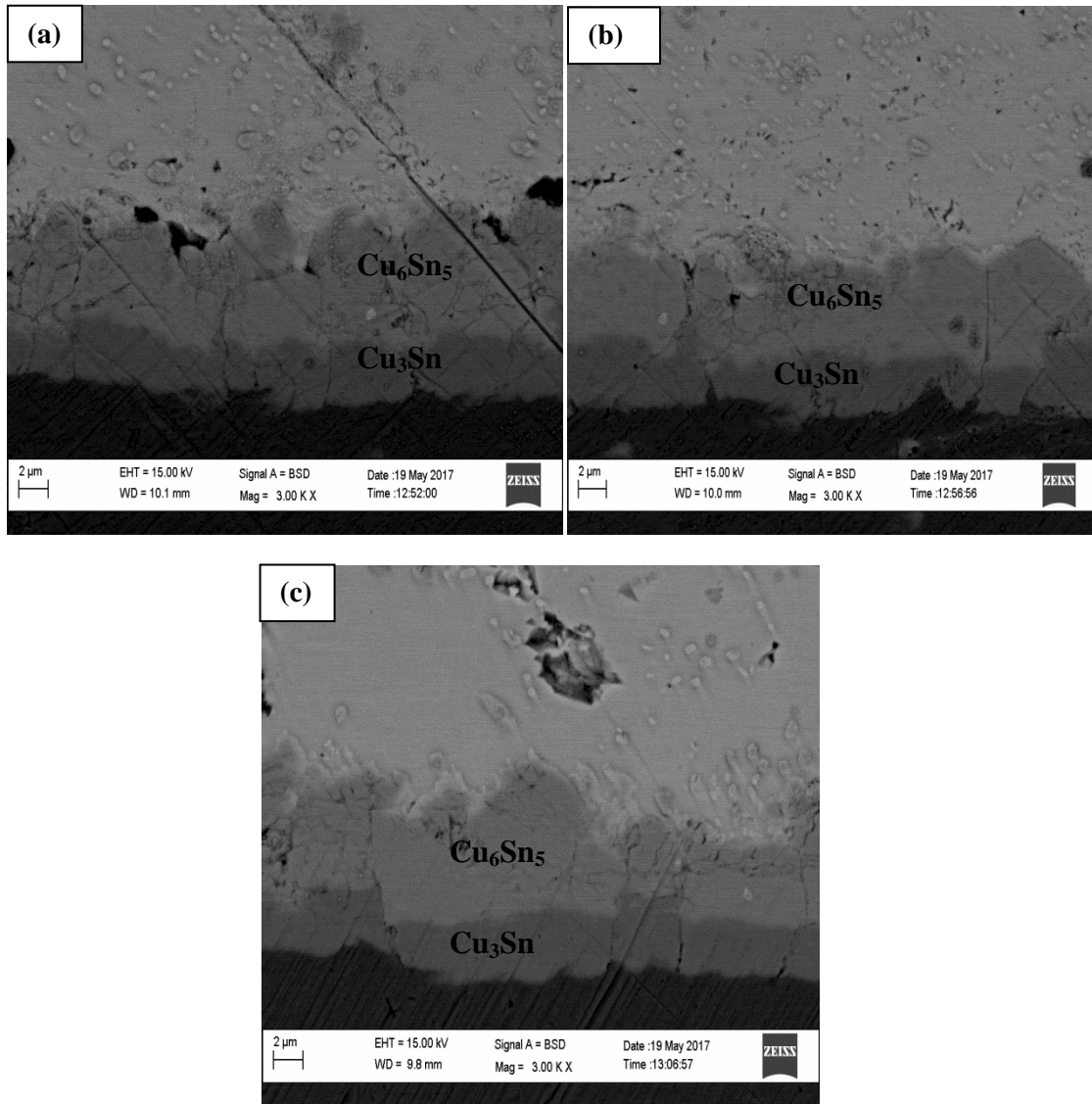


Figure 4.4 IMC layer at solder-substrate interface of route A ECAP for sample isothermally aged for 100 hours at 180°C (a) 0 pass (b) 4 passes and (c) 9 passes ECAPed solder alloys



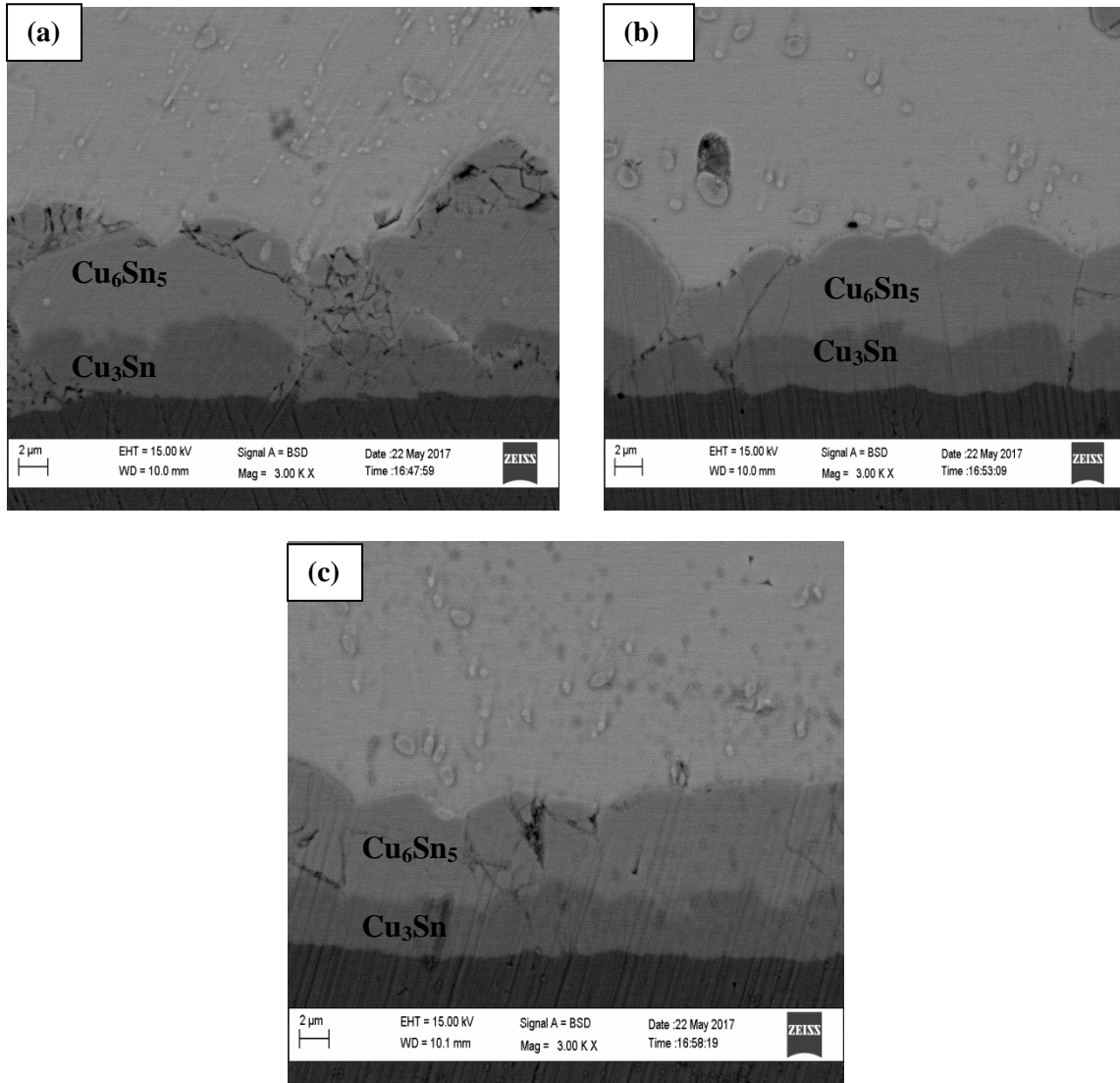


Figure 4.5 IMC layer at solder-substrate interface of route A ECAP for sample isothermally aged for 250 hours at 180°C (a) 0 pass (b) 4 passes and (c) 9 passes ECAPed solder alloys

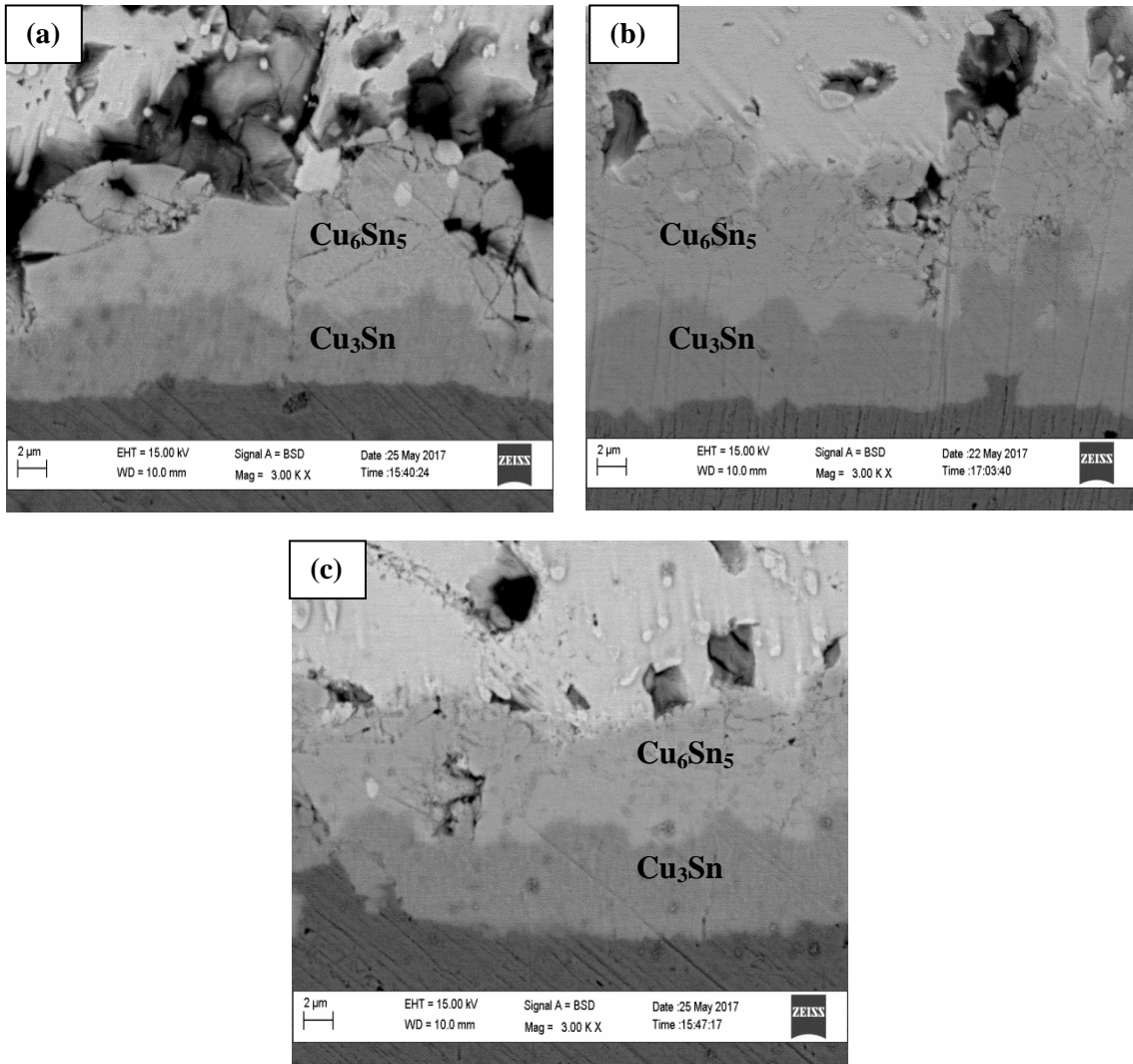


Figure 4.6 IMC layer at solder-substrate interface of route A ECAP for sample isothermally aged for 500 hours at 180°C (a) 0 pass (b) 4 passes and (c) 9 passes ECAPed solder alloys

Table 4.8 Thickness of IMC layer for as-reflowed sample and after isothermal aging

Condition	0 pass		4 passes		9 passes	
	t ( $\mu\text{m}$ )	$\Delta t/$ hours ( $\mu\text{m}/\text{h}$ )	t ( $\mu\text{m}$ )	$\Delta t/$ hours ( $\mu\text{m}/\text{h}$ )	t ( $\mu\text{m}$ )	$\Delta t/$ hours ( $\mu\text{m}/\text{h}$ )
As-reflowed	2.37	0	2.23	0	2.07	0
100h 180°C	4.12	0.0175	3.83	0.016	3.59	0.01520
250h 180°C	4.53	0.00164	3.97	0.00056	3.70	0.00044
500h 180°C	5.19	0.00132	5.01	0.00208	4.73	0.00206

The IMC layer for all samples with different ECAP passes displayed a significant growth after isothermal aging and finally thick IMC layer. The growth of interfacial IMC layer of isothermally aged sample occur due to enhanced diffusion with thermal energy which produces a driving force that causes growth of the IMC layer. The growth of interfacial IMC layer obeyed the Fick's Law Diffusion where IMC growth followed the parabolic growth kinetics. The longer the aging time, the IMC grows and forming a thicker layer. Apart from that, it can also be observed that there are two types of interfacial IMC layers present in isothermally aged samples. The two types of interfacial IMC layers are  $\text{Cu}_6\text{Sn}_5$  (the lighter area and located adjacent to the bulk solder) and  $\text{Cu}_3\text{Sn}$  IMC layer (the darker area and located adjacent to the Cu substrate). These two types of IMC have been commonly observed and reported by many researchers working on aging of Sn-based solder on Cu substrate.

#### 4.7 Tensile strength

Table 4.9 and Table 4.10 summarize the data analysis of tensile strength and number of ECAP passes of solder alloy before and after aging. When the number of ECAP passes increased, the tensile strength decreased. Figure 4.7 illustrate Scanning electron microscopy images on the fracture surface of solder joint after shear test. Figure 4.8 shows the surface morphology on fracture surface of reflowed solder during tensile test for different ECAP passes of 0 pass, 4 passes and 9 passes. From the morphology shown, the fracture surface shows brittle fracture. It can also be seen that sample of 9 passes has a higher amount of pores, followed by 4 passes and 0 pass. Therefore, this is the reason of 9 passes obtained lowest tensile strength among others because it has many pores compared to other passes. A study reported that, as thermal aging increases, the shear strength decreases. This can be judged as the thermal aging triggers the growth of Cu-Sn type IMC at interface and hence influences the value of shearing strength. Higher thermal aging produced pores and this results in a reduced shear strength and shows a tendency towards brittle fracture (Sharma et al. 2017) .

Table 4.9 Tensile strength (MPa) of ECAPed solder alloy before aging

Specimen	Sample		Average
	1	2	
0 pass	84.67	81.06	82.87
4 passes	36.82	31.49	52.57
9 passes	19.11	14.86	16.99

Table 4.10 Tensile strength (MPa) of ECAPed solder alloy after aging

Specimen	Sample		Average
	1	2	
0 pass	52.52	52.86	52.69
4 passes	33.19	20.64	26.92
9 passes	18.22	17.90	18.06

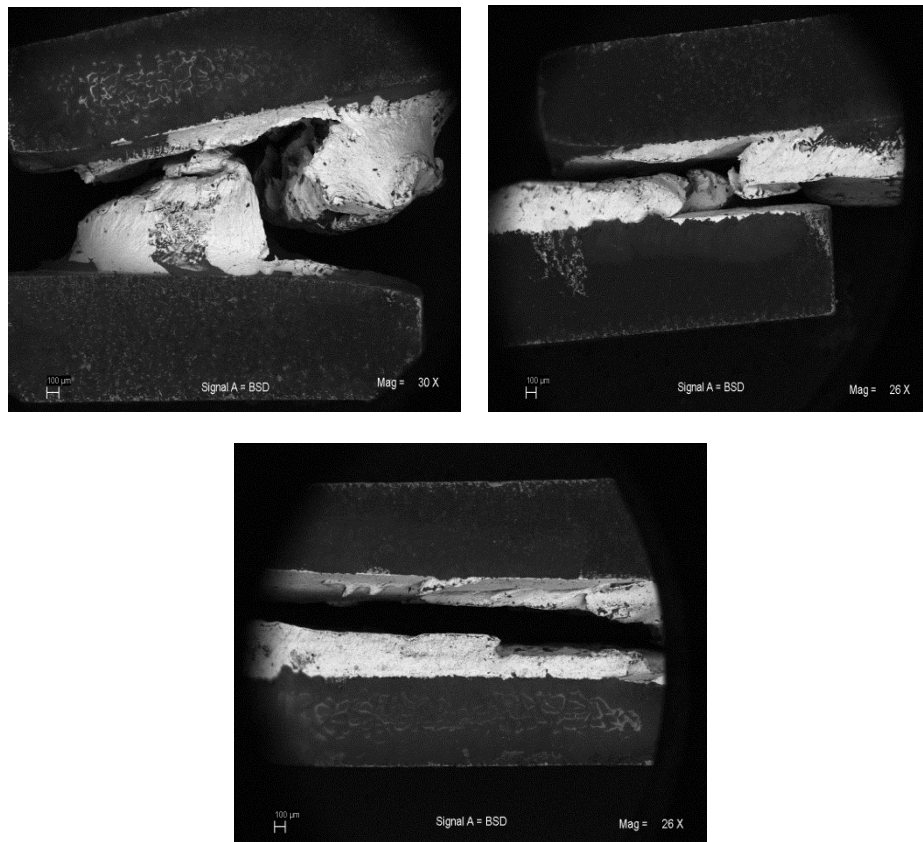


Figure 4.7 Scanning electron microscopy images on the fracture surface of solder joint after shear test

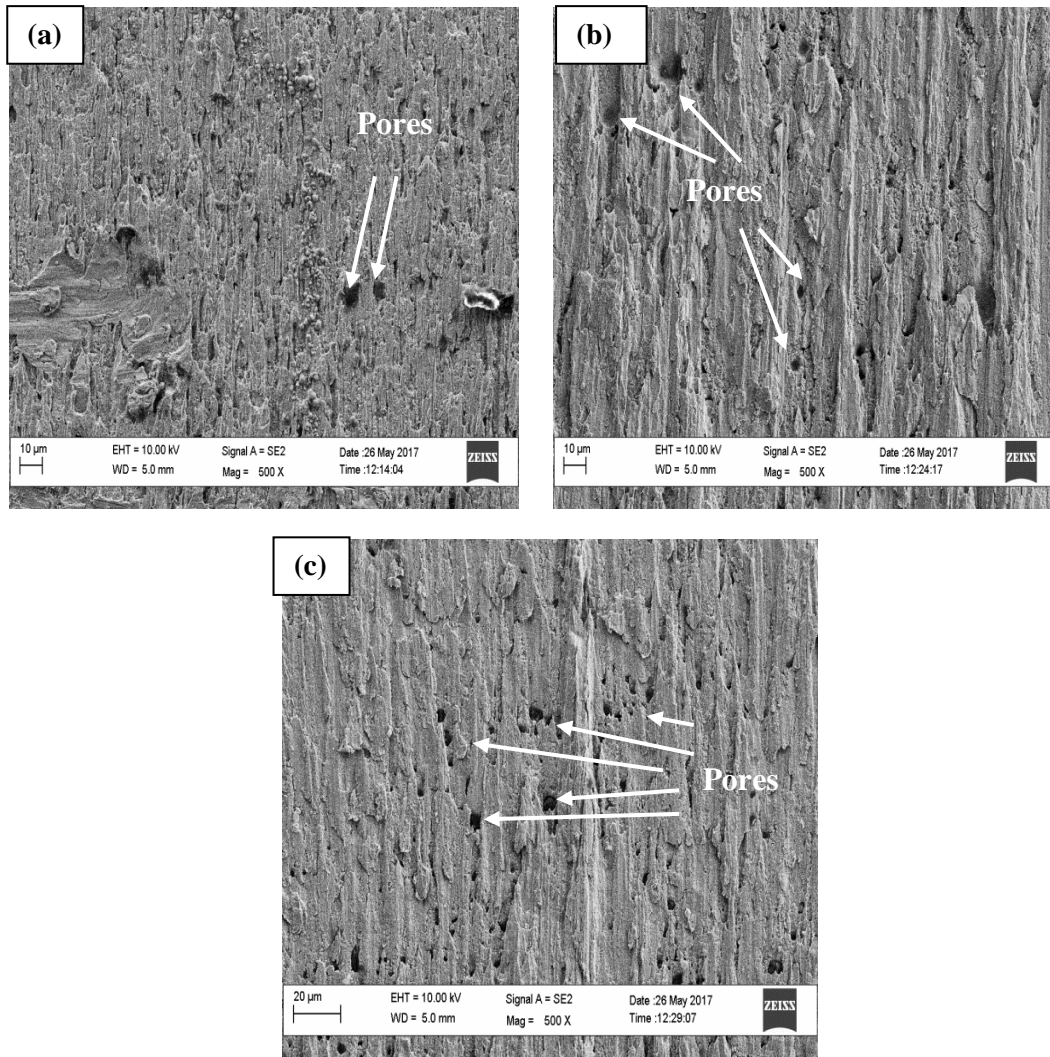


Figure 4.8 Surface morphology on fracture surface of reflowed solder during tensile test for different ECAP passes (a) 0 pass (b) 4 passes (c) 9 passes

## CHAPTER 5

### CONCLUSION AND RECOMMENDATION

#### 5.1 Conclusion

Sn-Ag-Cu is a leading ternary solder candidate system in soldering. It has advantages such as having lower melting point than Sn-Ag and Sn-Cu binary alloys and adequate wetting mechanical properties. However, in order to improve the mechanical properties of Sn-Ag-Cu solder alloy, a severe plastic deformation called ECAP has been performed. ECAP modifies the grain size from large  $\beta$ -Sn dendrites into finer  $\beta$ -Sn dendrites.

- 1) In this project, ECAP was observed to refine the  $\beta$ -Sn grains, which would improve the mechanical properties of Sn-Ag-Cu solder alloy. The hardness of bulk solder increased due to the formation of finer grains.
- 2) Besides, the thickness of interfacial of IMC layer during reflow and isothermal aging has reduced due to the plastic deformation of ECAP. More passes was applied on solder, more reduction on thickness of IMC layer. However, tensile strength of solder joint during reflow and isothermal aging decreased as increasing number of ECAP passes.

## 5.2 Recommendation

After carrying this project, several recommendations were made. ECAP processing involves process in which the process of pressing a billet along tool die with certain die angle and curvature angle. ECAP was handled manually where the die tool needed to be lifted up manually on UTM machine. Handling ECAP manually requires longer period of time to produced ECAPed sample. Further recommendation is to provide advance facilities on ECAP processing.

Besides, ECAP should use the most efficient route which is route B<sub>c</sub> in order to achieve effective result in modification of grain size from initially coarse grains into finer grains. Grain refinement would improve the mechanical properties of solder alloys. The number of passes should also be further increased to a higher level of passes in order to achieve much greater effect of ECAP.

In addition, in order to characterize the effect of ECAP on bulk solder and solder joint, another recommendation to be made is to add in another testing which is related such as solder ball shear and pull tests for solder ball application in order to prove the effect of ECAP on mechanical properties of solder alloy significantly.



## REFERENCES

- Berthou, M. et al. 2009. Microstructure evolution observation for SAC solder joint: Comparison between thermal cycling and thermal storage. *Microelectronics Reliability*, 49(9–11), pp.1267–1272.
- Chellvarajoo, S., Abdullah, M.Z. & Samsudin, Z., 2015. Effects of Fe<sub>2</sub>NiO<sub>4</sub> nanoparticles addition into lead free Sn-3.0Ag-0.5Cu solder pastes on microstructure and mechanical properties after reflow soldering process. *Materials and Design*, 67, pp.197–208.
- Djavanroodi, F. et al., 2012. Designing of ECAP parameters based on strain distribution uniformity. *Progress in Natural Science: Materials International*, 22(5), pp.452-460.
- El-Daly, A.A. et al., 2013. Microstructure, mechanical properties, and deformation behavior of Sn-1.0Ag-0.5Cu solder after Ni and Sb additions. *Materials and Design*, 43, pp.40–49.
- Frear, D.R. et al., 2001. Pb-free solders for flip-chip interconnects. *Journal of Materials Science*, 53(6), pp.28–33.
- Furukawa, M. et al., 2001. Review: Processing of metals by equal-channel angular pressing. *Journal of Materials Science*, 36(12), pp.2835–2843.
- Gao, L. et al., 2010. Effect of alloying elements on properties and microstructures of SnAgCu solders. *Microelectronic Engineering*, 87(11), pp.2025–2034.
- Jain, V. et al., 2014. Micromanufacturing: A review--part II. *Proceedings of the Institution of Mechanical Engineers, Part B: Journal of Engineering Manufacture*, 228(9), pp.995–1014.

Keller, J. et al., 2011. Mechanical properties of Pb-free SnAg solder joints. *Acta Materialia*, 59(7), pp.2731–2741.

Kim, K.S., Huh, S.H. & Suganuma, K., 2003. Effects of intermetallic compounds on properties of Sn-Ag-Cu lead-free soldered joints. *Journal of Alloys and Compounds*, 352(1–2), pp.226–236.

Lin, J. et al., 2009. Microstructure and high tensile ductility of ZK60 magnesium alloy processed by cyclic extrusion and compression. *Journal of Alloys and Compounds*, 476(1–2), pp.441–445.

Morando, C. et al., 2012. Microstructure evolution during the aging at elevated temperature of Sn-Ag-Cu solder alloys. *Procedia Materials Science*, 1, pp.80–86.

N, E.E.M. & A, A.M., 2012. A review of solder evolution in electronic application. *International Journal of Engineering*, 1(1), p.2305–8269.

Nadhirah, M.K.N. et al., 2016. Isothermal Aging of Low-Ag SAC with Al Addition. *Procedia Chemistry*, 19, pp.492–497.

Piyavatin, P., Lothongkum, G. & Lohwongwatana, B., 2012. Characterization of eutectic Sn-Cu solder alloy properties improved by additions of Ni, Co and in. *Materials Testing*, 54(6), pp.383–389.

Sanusi, K.O., Makinde, O.D. & Oliver, G.J., 2012. Equal channel angular pressing technique for the formation of ultra-fine grained structures. *South African Journal of Science*, 108(9–10), pp.1–7.

Shaeri, M.H. et al., 2015. Effect of equal channel angular pressing on aging treatment of Al-7075 alloy. *Progress in Natural Science: Materials International*, 25(2), pp.159–168.

Sharma, A. et al., 2017. Thermal cycling, shear and insulating characteristics of epoxy embedded Sn-3.0Ag-0.5Cu (SAC305) solder paste for automotive applications. *Journal of Alloys and Compounds*, 704, pp.795–803.

Tschopp, M.A. & McDowell, D.L., 2008. Grain boundary dislocation sources in nanocrystalline copper. *Scripta Materialia*, 58(4), pp.299–302.

Vafaenezhad, H. et al., 2016. Workability Study in Near- Peritectic Sn-5 % Sb Lead-Free Solder Alloy Processed By Severe Plastic Deformation. , 3(2), pp.39–51.

Verlinden, B., 2009. Severe plastic deformation of metals. *Metalurgija-Journal of Metallurgy*, 44(2002), pp.1900–1911.

Xiao, Q.X.Q., Nguyen, L.N.L. & Armstrong, W.D., 2004. Aging and creep behavior of Sn3.9Ag0.6Cu solder alloy. *2004 Proceedings. 54th Electronic Components and Technology Conference (IEEE Cat. No.04CH37546)*, 2, pp.1325–1332.

Yasmin, T., Sadiq, M. & Khan, M.I., 2014. Effect of Lanthanum Doping on the Microstructure Evolution and Intermetallic Compound ( IMC ) Growth during Thermal Aging of SAC305 Solder Alloy. *Material Science & Engineering*, 3(2),

pp.1-8.

Zhu, C.F. et al., 2013. Microstructure and strength of pure Cu with large grains processed by equal channel angular pressing. *Materials and Design*, 52, pp.23–29.

Zhu, Q.S. et al., 2009. Enhanced rate-dependent tensile deformation in equal channel angularly pressed Sn-Ag-Cu alloy. *Materials Science and Engineering A*, 502(1–2), pp.153–158.

Zhu, Y.T. & Lowe, T.C., 2000. Observations and issues on mechanisms of grain refinement during ECAP process. *Materials Science and Engineering A*, 291(1), pp.46–53.

Zrnik, J., Dobatkin, S. & Mamuzic, I., 2008. Processing of metals by severe plastic deformation (SPD)-structure and mechanical properties respond. *Metalurgija*, 47(3), pp.211–216.